

University of Windsor

Scholarship at UWindor

Electronic Theses and Dissertations

Theses, Dissertations, and Major Papers

2013

Plasma Electrolytic Oxidation (PEO) Coatings on an A356 Alloy for Improved Corrosion and Wear Resistance

Zhijing Peng
University of Windsor

Follow this and additional works at: <https://scholar.uwindsor.ca/etd>

Recommended Citation

Peng, Zhijing, "Plasma Electrolytic Oxidation (PEO) Coatings on an A356 Alloy for Improved Corrosion and Wear Resistance" (2013). *Electronic Theses and Dissertations*. 4764.
<https://scholar.uwindsor.ca/etd/4764>

This online database contains the full-text of PhD dissertations and Masters' theses of University of Windsor students from 1954 forward. These documents are made available for personal study and research purposes only, in accordance with the Canadian Copyright Act and the Creative Commons license—CC BY-NC-ND (Attribution, Non-Commercial, No Derivative Works). Under this license, works must always be attributed to the copyright holder (original author), cannot be used for any commercial purposes, and may not be altered. Any other use would require the permission of the copyright holder. Students may inquire about withdrawing their dissertation and/or thesis from this database. For additional inquiries, please contact the repository administrator via email (scholarship@uwindsor.ca) or by telephone at 519-253-3000ext. 3208.

**Plasma Electrolytic Oxidation (PEO) Coatings on
an A356 Alloy for Improved Corrosion and Wear
Resistance**

by
Zhijing Peng

Thesis
Submitted to the Faculty of Graduate
Studies through Engineering Materials
in Partial Fulfillment of the
Requirements for the Degree of Master
of Applied Science at the University of
Windsor

Windsor, Ontario, Canada

2013

©2013 Zhijing Peng

Plasma Electrolytic Oxidation (PEO) Coatings on an A356 Alloy
For Improved Corrosion and Wear Resistance

by

Zhijing Peng

APPROVED BY:

Dr. H. Wu

Department of Electrical and Computer Engineering

Dr. H. Hu

Department of Mechanical, Automotive and Materials Engineering

Dr. X. Nie, Advisor

Department of Mechanical, Automotive and Materials Engineering

Dr. V. Stoilov, Chair of Defense

Department of Mechanical, Automotive and Materials Engineering

27 February 2013

DECLARATION OF CO-AUTHORSHIP/PREVIOUS PUBLICATION

I. CO- AUTHORSHIP DECLARATION

I hereby declare that this thesis incorporates material that is result of joint research, as follows:

This thesis incorporates the outcome in collaboration with Dr. Yin Chen for SEM pictures and samples preparation under the supervision of Professors Xueyuan Nie. The collaboration is covered in Chapter 4 of the thesis. This thesis also incorporates the outcome in collaboration with Dr. Tse Cheng for roughness measurement under the supervision of Professors Xueyuan Nie. The collaboration is covered in Chapter 6 of the thesis. In all cases, the key ideas, primary contributions, experimental designs, data analysis and interpretation, were performed by the author, and the contribution of the co-author was primarily through the provision of experiments.

I am aware of the University of Windsor Senate Policy on Authorship and I certify that I have properly acknowledged the contribution of other researchers to my thesis, and have obtained written permission from each of the co-author(s) to include the above material(s) in my thesis.

I certify that, with the above qualification, this thesis, and the research to which it refers, is the product of my own work.

II. DECLARATION OF PREVIOUS PUBLICATION

This thesis includes 4 original papers that have been previously published/submitted for publication in peer reviewed journals/conference proceedings, as follows:

Thesis Chapter	Publication title/full citation	Publication status
Chapter 4	Zhijing Peng, Ying Chen and Xueyuan Nie, Corrosion properties of plasma electrolytic oxidation ceramic coatings on an A356 alloy tested in an ethanol-gasoline fuel (E85) medium. <i>Advanced Materials Research, Vols. 282-283 (2011) pp 774-778</i>	Published
Chapter 5	Z. Peng and X. Nie, Galvanic corrosion property of contacts between carbon fiber cloth materials and typical metal alloys in an aggressive environment. <i>Surface & Coatings Technology, 215 (2013) 85-89</i>	Published
Chapter 6	Zhijing Peng, Tse Cheng and Xueyuan Nie, MoS ₂ /Al ₂ O ₃ composite coatings on A356 alloy for friction reduction. <i>Advanced Materials Research, Vol. 496 (2012) pp 488-492</i>	Published
Chapter 7	Zhijing Peng and Xueyuan Nie, Effect of plasma electrolytic oxidation coatings on friction and wear behavior of aluminum engine cylinder bores. <i>Surface & Coatings Technology, to be submitted</i>	Proceed

I hereby certify that I have obtained a written permission from the copyright owner(s) to include the above published material(s) in my dissertation. I certify that the above material describes work completed during my registration as graduate student at the University of Windsor.

I declare that, to the best of my knowledge, my thesis does not infringe upon anyone's copyright nor violate any proprietary rights and that any ideas, techniques, quotations, or any other material from the work of other people included in my dissertation, published or

otherwise, are fully acknowledged in accordance with the standard referencing practices. Furthermore, to the extent that I have included copyrighted material that surpasses the bounds of fair dealing within the meaning of the Canada Copyright Act, I certify that I have obtained a written permission from the copyright owner(s) to include such material(s) in my dissertation. I declare that this is a true copy of my thesis, including any final revisions, as approved by my dissertation committee and the Graduate Studies office, and that this thesis has not been submitted for a higher degree to any other University or Institution.

ABSTRACT

Plasma electrolytic oxidizing (PEO) is an advanced technique that has been used to deposit thick and hard ceramic coatings on aluminium (Al) alloys. This work was however to use the PEO process to produce thin ceramic oxide coatings on an A356 Al alloy for improving corrosion and wear resistance of the alloy. Effects of current density and treatment time on surface morphologies and thickness of the PEO coatings were investigated. The improvement of galvanic corrosion properties of the coated A356 alloy vs. steel and carbon fibre were evaluated in E85 fuel or NaCl environments. Tribological properties of the coatings were studied with comparison to the uncoated A356 substrate and other commercially-used engine bore materials. The research results indicated that the PEO coatings could have excellent tribological and corrosion properties for aluminium engine applications.

DEDICATION

I would like to dedicate this dissertation to my parents for their unconditional love, support and encouragement.

I also would like to thank my wife. Her love and support enable me to go through the difficult time and finally complete this thesis.

ACKNOWLEDGEMENTS

This study could not have done forward without the financial support from the Natural Sciences and Engineering Research Council of Canada (NSERC).

I would like to thank my thesis advisor, Dr. Xueyuan Nie, for his valuable suggestions and excellent supervision of this research work during my study.

Many thanks to my committee members (Dr. Henry Hu, Dr. Huapeng Wu) for their helpful comments and careful review of this work.

I would like to thank Mr. Junfeng Su, Mrs. Ying Chen, Mr. Rayid Hussin and Dr. Tse Cheng from University of Windsor for their assistance with the experiments.

Finally, I am thankful to the faculty, staff and graduate students at the Department of Mechanical, Automotive and Materials Engineering of the University of Windsor, particularly my colleagues at the PEO lab, for their support and encouragement.

TABLE OF CONTENTS

DECLARATION OF CO-AUTHORSHIP/PREVIOUS PUBLICATION	III
ABSTRACT	VI
DEDICATION	VII
ACKNOWLEDGEMENTS	VIII
LIST OF TABLES	XI
LIST OF FIGURES	XII
CHAPTER 1 INTRODUCTION	1
REFERENCES.....	9
CHAPTER 2 LITERATURE REVIEW	12
1. The PEO equipment	13
2. Deposition procedure.....	14
3. PEO coating structure.....	16
4. Tribological properties of PEO coatings.....	17
5. General corrosion characteristics of Al alloys.....	20
6. Summary of literature review.....	23
REFERENCES.....	24
CHAPTER 3 EXPERIMENTAL PROCEDURES	28
1. Pin-on-disc/reciprocating tribology test.....	28
2. Potentiodynamic polarization testing.....	29
3. Zero Resistance Ammetry.....	32
REFERENCES.....	33
CHAPTER 4 CORROSION PROPERTIES OF PLASMA ELECTROLYTIC OXIDATION CERAMIC COATINGS ON AN A356 ALLOY TESTED IN AN ETHANOL-GASOLINE FUEL (E85) MEDIUM	34
1. Introduction.....	34
2. Experiments.....	35
3. Results.....	36
4. Conclusion	40
REFERENCES.....	41

CHAPTER 5 GALVANIC CORROSION PROPERTY OF CONTACTS BETWEEN CARBON FIBER CLOTH MATERIALS AND TYPICAL METAL ALLOYS IN AN AGGRESSIVE ENVIRONMENT.....	43
1. Introduction	43
2. Experimental details.....	45
3. Results and discussion	47
4. Conclusions	55
REFERENCES.....	56
CHAPTER 6 MOS₂/AL₂O₃ COMPOSITE COATINGS ON A356 ALLOY FOR FRICTION REDUCTION.....	58
1. Introduction	58
2. Experimental procedure.....	59
3. Results and Discussion.....	61
4. Conclusions	64
REFERENCES	65
CHAPTER 7 EFFECT OF PLASMA ELECTROLYTIC OXIDATION COATINGS ON FRICTION AND WEAR BEHAVIOR OF ALUMINUM ENGINE CYLINDER BORES.....	66
1. Introduction.....	66
2. Experiment method.....	68
3. Result and Discussion.....	70
4. Conclusions	83
REFERENCES	84
CHAPTER 8 SUMMARY AND FUTURE WORKS.....	87
1. Summary.....	87
2. Future work.....	90
APPENDIX COPYRIGHT RELEASES FROM PUBLICATIONS.....	91
VITA AUCTORIS	99

LIST OF TABLES

Table 4.1. Potentiodynamic polarization parameters of uncoated/coated A356 and steel in E85.....	37
Table 5.1. Potentiodynamic polarization parameters of uncoated/coated A356 and steel in a NaCl solution and thickness of alumina coatings.....	47

LIST OF FIGURES

Figure 2.1 Typical arrangement of the equipment used for PEO treatment.....	14
Figure 2.2 Current-voltage diagram for the processes of plasma electrolysis: discharge phenomena are developed in the dielectric film on the electrode surface.....	15
Figure 2.3 Illustrates the structure of the PEO coating.....	16
Figure 2.4 Segmented Ring/Bore Liner test rig.....	19
Figure 2.5 Potentiodynamic polarization curves of untreated substrate materials and PEO alumina coatings in 0.5M NaCl solution after different immersion times.....	22
Figure 3.1 Sliding tester attached on (a) Sciland Pin/Disc Tribometer PCD-300A, (b) load cell and cantilever beam, (c) sample holder for reciprocating mode and (d) sample holder plus load.....	28
Figure 3.2 Typical polarization curve.....	30
Figure 3.3 Theoretical cathodic polarization scan.....	31
Figure 3.4 Tafel slope calculation.....	31
Figure 3.5 (a) Schematic view of three-electrode cell and (b) Electrochemical corrosion polarization testing equipment, (c) General galvanic corrosion test and (d) ZRA test... ..	33
Figure 4.1 Cross sectional SEM micrographs of samples A-D coatings.....	37
Figure 4.2 Potentiodynamic polarization corrosion curves of the samples in an E85 medium.....	38
Figure 4.3 The galvanic corrosion current density of the test samples in the E85 medium	39
Figure 4.4 SEM micrographs of (a, b) uncoated A356, (c) Sample C and (d) Sample D after	

ZRA corrosion tests.....	40
Figure 5.1 Optical images of (a) ASTM A1018 steel, (b) aluminum alloy A356 and (c) Ti6Al4V alloys after corrosion tests. Inserts in (a), (b) and (c) showed the corroded areas at a low magnification.....	48
Figure 5.2 Potentiodynamic polarization corrosion curves of the samples in a 3.5% NaCl solution. Treatment modes for samples: A- bipolar, B- unipolar/bipolar, C bipolar/unipolar, D- unipolar.....	49
Figure 5.3 The galvanic corrosion current density curves of the test samples in the 3.5% NaCl solution for (a) all samples and (b) samples A, B and D at a magnified scale. A -bipolar, B-unipolar/bipolar, C-bipolar/unipolar, D-unipolar.....	52
Figure 5.4 SEM micrographs of (a. b) uncoated A356, (c) Sample B and (d) Sample C after ZRA corrosion tests.....	53
Figure 5.5 The optical micrographs and galvanic corrosion current density of the test samples in the 3.5% NaCl solution for Ti6Al4V alloys: (a) uncoated, (b) treated by a bipolar current mode (TB) and (c) treated by a unipolar mode.....	54
Figure 6.1 C.O.F. curves of (a) A356, S1 and S2 and (b) S3, S4 and S5 at 2N & 50m dry test conditions.....	61
Figure 6.2 C.O.F. curves of (a) S1 and (b) S5 at 1N and 50m dry test conditions.....	62
Figure 6.3 SEM micrographs and EDX spectra of coatings on (a, b) Sample 1 (without MoS ₂) and (c. d) Sample 5 (with MoS ₂).....	63
Figure 6.4 (a) Wear rates of samples S1 and S2 under the pin-on-disc dry test conditions for both 2N and 1N (labeled with*) loads, and (b) tribological behaviours of A356 and coated samples under lubricant test conditions at a 2N load for 50m (4000 revolutions).....	63

Figure 7.1 Optical micrographs of (i) the wear tracks on PEO coatings and (ii) wear scars on counterface steel balls, and (iii) C.O.F. for (a) Coating S1, (b) Coating S2, and (c) Coating S3.72

Figure 7.2 Optical micrographs of (i) the wear tracks on reference samples and (ii) wear scars on counterface steel balls, and (iii) C.O.F. for (a) PTWA coating, (b) Alusil, and (c) cast iron.....75

Figure 7.3 SEM micrographs for (a, b) PWTA, (c-d) Alusil and (e-f) cast iron liner specimen after the tribotest.....79

Figure 7.4 SEM micrographs and EDX spectra of the coating S2 after tested at a 15N, 1000m and oil lubricant condition.....80

Figure 7.5 SEM micrographs and EDX spectra of the coating S1 after tested at a 15N, 1000m and oil lubricant condition..... 81

Figure 7.6 Optical images of (a) the coating S1 and (b) counter-ball as well as (c) PTWA coating and (d) counter-ball. (e) C.O.F curves for the coatings.82

CHAPTER 1

INTRODUCTION

Recently, environmental problems caused by fuel emissions and limited fuel supplies force the automotive industry to use new lightweight materials. The need to improve fuel economy and safety performance, reduce exhaust emissions and provide customers with new features have caused new renovations in components design including reduced friction, weight, and higher engine operating temperatures for improved efficiency. To achieve such an objective, aluminium (Al) alloys are noted for their unique combination of desirable characteristics including their high strength-to-weight-ratio, good castability, low thermal expansion and high corrosion resistance. These properties have led to their increase sufficiently in the use of automotive besides aircraft and aerospace industry. Aluminum-silicon (AlSi) alloys such as Al 356 [1] have been commercially used to produce engine blocks because of its high strength over weight ratio. The engine block cylinder works under thermal and mechanical cyclic stresses in relative motion with piston rings. It is shown that good wear resistance is a critical property to engine block's working life. Although aluminum alloys are becoming increasingly important, and more widely used in the automobile industry due to their excellent properties, including high strength to weight ratio, good castability and machinability their corrosion resistance is relatively poor because of the presence of non-corrosion resistant elements and phases (Cu, Si, Mg, etc) and microstructural defects (such as pores) in these alloys. Many industrial approaches to improving corrosion resistance have been taken including the development of new alloy systems, the use of inhibitors, and surface modification to change the chemistry, composition and properties of the alloy surface [2].

A356 series cast aluminium-silicon alloys have been increasingly applied as lightweight components especially using for all types of internal combustion engines as pistons, cylinder blocks and cylinder heads. In this kind of alloys, silicon is added to aluminium and can be used to form a second phase in order to improve wear resistance for tribological applications. However, compared with steel and iron, aluminium alloys such as A356 are relatively soft and have poor wear properties especially against scuffing wear under conditions of dry lubrication such as those which exist during starting engines period. It is one of the failure mechanisms affecting the useful life of engines. [3-5] Also the National Ethanol Vehicle Coalition (NEVC) and the Petroleum Equipment Institute have pointed out that aluminum alloy is sensitive to corrosion from ethanol. The use of corrosive ethanol such as E85 can be accommodated through the use of appropriate coatings, valve seat materials, adhesives, and fuel additives [6].

Surface coating can be used to minimize the possibility of sever wear by lowing friction and hardening the surface. Various coatings have been developed to improve wear properties of the alloys. Titanium nitride and diamond-like carbon (DLC) coatings are deposited by vacuum vapour deposition (PVD and CVD) methods which need high vacuum in vacuum chambers [7-8]. Electroplating and electroless plating-Nickel based ceramic composite coatings (NCC) have a function to increase the wear resistance but could be corroded when sulphur-contained fuel is used [9]. Thermal spraying technology can produce Fe-based or stainless steel-Ni-BN coatings. However, thermal spraying only make mechanical adhesion of coatings to base materials, and precise process control (including surface pre-treatment) is hard for good adhesion between coating and Al samples [10]. Manufacturing challenges still exist in producing spraying-coated

Al cylinder interior surfaces in terms of economical manufacturing process, reproducible and reliable processing. Hard anodizing is an effective and equipment simple method used to produce hard ceramic coatings on aluminium alloys. Since alloying elements such as copper and silicon do not anodize during the process, leaving microscopic voids in the aluminum oxide coating, the coating exhibits a low peeling resistance and high friction coefficient. In general case, hard anodic coatings are not suitable to be used to high Si (containing >8% silicon) alloys. [11]

For corrosion application, several surface modification and coating techniques have been developed to enhance the corrosion resistance of Al alloys. These techniques are sol-gel coatings [12-13], ion implantation [13-15], conversion coatings [16], physical vapor deposition (PVD) [17-20] chemical vapor deposition (CVD), and thermal spraying [21]. However, most of these methods involve high temperatures during processing (CVD, PVD and thermal spray) or post-treatment (sol-gel), which may damage the coating and /or substrate [22]. In addition, sol-gel processing has been of limited use due to poor interfacial adhesion, shrinkage and oxidation of the substrate [23]. Conversion coatings are mainly based on chromium compounds that exhibit good corrosion resistance, but have also been reported to be highly toxic and carcinogenic [23]. Ion implantation has found limited success in increasing the pitting potential of coatings.

Plasma electrolytic oxidation (PEO) is a relatively new plasma-assisted electrochemical treatment which is considered as a cost-effective and environmentally friendly surface engineering technique and can be broadly applied to metal surface cleaning, metal-coating [24], carburizing, nitriding [25], and oxidizing [26-29].

A PEO process in a silicate solution can produce Al-Si-O ceramic coatings with a high adhesion, hardness, and thickness on Al-based materials. Also, the PEO process combining with other processes such as CVD [30] and electrophoretic deposition (EPD) [31] can be used in producing super hard, low friction, and biomedical compatible coatings.

Several studies have been involved in the coating formation mechanisms [32-34], characteristics of the coating deposition including tribological properties [27-29] of the ceramic oxide coatings deposited using PEO on various Al alloy substrates. However, most of those works focused on 2xxx and 6xxx series, i.e., low silicon (<1.5% Si) content Al alloys, and characterized thick oxide coating (i.e., >100 μm in thickness). Little studies focus on the initial stage of the PEO coating formation and properties of the thin PEO coatings (i.e., < 50 μm). Due to the rapid growth in applications of high silicon cast Al-Si alloys, the applications of the PEO on the cast Al-Si alloys have been paid more attention since recently [35, 36]. However, to our knowledge, a detailed investigation of the effects of silicon content in Al-Si alloys such as A356 alloy on the PEO coating formation and morphology has not been conducted yet.

The global fuel crises in the 1970s triggered awareness in many countries of their vulnerability to oil embargoes and shortages. Considerable attention was focused on the development of alternative fuel sources, in particular, the alcohols [37]. Because it is a renewable bio-based resource and is oxygenated, ethyl alcohol is considered an attractive alternative fuel to reduce both the consumption of crude oil and environmental pollution. If ethanol from biomass is used to drive a light-duty vehicle, the net CO_2 emission is less than 7% of that from the

same car using reformulated gasoline [38]. Currently, ethanol is blended with gasoline to form an E10 blend (10% ethanol and 90% gasoline by volume), but it can be used in higher concentrations such as E85 or E95. In the past few years, automotive manufacturers have developed flexible fuel vehicles (FFVs) that can run on E85 fuel or any other combination of ethanol and gasoline [6].

Carbon fibers which will be used as commercial vehicle's bodies in the future years and aluminum alloys which can be used as chassis on future vehicles have created considerable interest as structural engineering materials and in many applications carbon fiber composite materials are connected to aluminum metals. When carbon fibers in a polymer based matrix composite are used as a structural component, it should be noted that carbon fiber is a very efficient cathode and very noble in the galvanic series. Therefore, contact between carbon fiber composites and metals in an electrolyte such as rain or seawater will be extremely undesirable if the metal is highly active and low in the galvanic series. If galvanic coupling occurs, galvanic corrosion of the metal may occur. Additional possibilities of corrosion related to raising the galvanic potential, particularly for passive metals such as aluminum alloys include: initiation of pitting corrosion and extensive crevice corrosion. [39, 40]

Thus, in this thesis, low voltages (<500V) were adopted to produce thin PEO coating with thickness less than 50 μm . The PEO process on aluminium alloys A356 (~7%Si) was investigated in terms of electrical and electrolytic parameters on formation, morphology, composition of the PEO coatings. Potentiodynamic polarization and Zero Resistance Ammetry (ZRA) corrosion testing methods were used to evaluate the corrosion properties of coated and

uncoated Al alloys (A356) in an alternative fuel. Effects of the current modes on the coating morphologies and anti-corrosion performance were particularly discussed in one of the chapters in this thesis. Also, the galvanic corrosion between metals and a carbon fiber sheet were investigated. In order to investigate the possibility and intensity of galvanic corrosion, not only potentiodynamic polarization but also zero resistance ammeter (ZRA) testing methods were used to evaluate the corrosion properties of a steel and a titanium alloy as well as coated and uncoated Al alloys (A356) in 3.5% NaCl solutions. As a result of this study, a better understanding of the galvanic corrosion behavior of the carbon fiber-metal system can be achieved.

For improved friction and anti-wear properties, PEO coatings plus MoS₂ particles has been applied to the A356 alumina alloy through the electrophoretic deposition of MoS₂ particles. The alkaline electrolyte solution containing suspension of MoS₂ particles was used to prepare a composite film of MoS₂ and Al₂O₃. The resulting microstructural and tribological properties were examined via optical microscopy, scanning electron microscopy (SEM) and tribotests. A reciprocating sliding tribometer was used to investigate the tribological and wear behavior of the PEO coatings and counterface materials, compared with plasma transferred wire arc coating, Alusil[®] and Casting Iron samples, under dry and lubricated conditions.

Objective and contents of this study

The objectives of this study were to:

1. Develop plasma electrolytic oxidation (PEO) coatings on an A356 aluminium alloy for its corrosion and wear prevention.
2. Investigate the possibility and intensity of galvanic corrosion of coated and uncoated Al alloys A356 vs. steel valve seats in E85 fuels and 3.5% NaCl solutions; investigate the galvanic corrosion behavior of the carbon fiber against coated A356 compared to uncoated A356, steel and Ti alloy; study the effects of the current modes on the coating morphologies and anticorrosion performance.
3. Optimize the PEO process for improved friction and anti-wear properties; investigate the tribological and wear behavior of the PEO coatings and counterface materials, compared with plasma transferred wire arc coating, Alusil[®] and casting iron samples, under dry and lubricated conditions.

Organization of the thesis

This thesis contains eight chapters. Chapter 1 gives introductory information on the usage of A356 aluminium alloy in automotive applications and the need for improved corrosion and wear resistance. Following this introduction, the relevant literatures regarding PEO coating technology on Al alloys and previous research on the PEO coating formation and properties are reviewed in Chapter 2. Chapter 3 describes the experimental instruments and procedures. Chapter 4 reports investigation results of corrosion property of plasma electrolytic oxidation coatings tested in an ethanol gasoline fuel (E85) medium. Chapter 5 presents the results and discussion of the corrosion property of contacts between carbon fiber cloth materials and typical metal alloys with

and without PEO coatings. In chapter 6, a new $\text{Al}_2\text{O}_3/\text{MoS}_2$ composite coating was developed, and its tribological properties were investigated under dry and lube conditions. Chapter 7 presents wear and friction properties of the PEO coating on engine bores, compared with commercial engine block materials. Chapter 8 is to summarize the research results of this thesis and also provide suggestion of future work.

References

- [1] A.M. Sherman, in E.A. Starke, Jr., T.H. Sanders, Jr., W.A. Cassada (ed.), Aluminium alloys: their physical and mechanical properties, Vol. 331-337, Part 1, Trans tech publications Ltd., 2000, p3-4.
- [2] Y. Sun, Materials Letters 58 (2004) 2635-2639
- [3] R Shivanath, P.K. Sengupta, Eyre T S, The British Foundryman, 70 (1977), 349-356.
- [4] A.S. Reddy, B.N.P Bai, K.S.S. Murthy, S.K. Biswas, Wear, 171 (1994), 115-127.
- [5] B.S. Shabel, D.A. Granger, W.G. Truckner, in D. Olson Hardbound (ed.), ASM Handbook, Vol. 18, 1992, p785-794.
- [6] Handbook for Handling, Storing, and Dispensing E85, 2002
http://www.e85fuel.com/pdf/ethanol_guidebook.pdf
- [7] J. W Cox, in R.F. Bunshah (ed.), Handbook of Hard Coatings, William Andrew Publishing, 2001, p420-457.
- [8] Y.C. Wang, S.C. Tung, Wear, 225-229 (1999), 1100-1108.
- [9] A.E. Ostermann, Experiences with Nickel-Silicon Carbide Coatings in Cylinder Bores of Small Aluminum Engines, TP 790843, Society of Automotive Engineers, 1979.
- [10] A. Edrisy, T. Perry, Y.T. Cheng, A.T. Alpas, Wear, 251 (2001), 1023-1033.
- [11] Ronald A. Walsh, Electromechanical Design Handbook (3rd Edition), McGRAW-HILL, New York (2000), p13.15.
- [12] M. Sheffer, A. Groysman, D. Mandler, Corrosion Science 45 (2003) 2893-2904.
- [13] J. Masalski, J. Gluszek, J. Zabrzski, K. Nitsch, P. Gluszek, Thin Solid Films 349 (1-2) (1999) 186-190.

- [14] X. Zhang, S. Lo Russo, S. Zandolin, A. Miotello, E. Cattaruzza, P.L. Bonora, L, Corrosion Science 43 (2001) 85-97.
- [15] P. Preston, R. Smith, A. Buchanan, J.M. Williams, Scripta Metallurgica et Materialia 32 (1995) 2021-2027.
- [16] J. Zhao, L. Xia, A. Sehgal, D. Lu, R.L. McCreery, G.S. Frankel, Surface and Coatings Technology 140(2001) 51-57.
- [17] C. Taschner, B. Ljungberg, V. Alfredsson, I. Endler, A. Leonhardt, Surface and Coatings Technology 109 (1998) 257-264.
- [18] A. Larsson, M. Halvarsson, S. Rупpi, Surface and Coatings Technology 111 (1999) 191-198.
- [19] J.M. Schneider, W.D. Sproul, A.A. Voevodin, A. Matthews, Journal of Vacuum Science and Technology A- Vacuum, Surfaces, and Films Part15 (1997) 1084-1088.
- [20] D.E. Ashenford, F. Long, W.E. Hagston, B. Lunn, A. Matthews, Surface and Coatings Technology 119 (1999) 699-704.
- [21] B.H. Kear, Z. Kalman, R.K. Sadangi, G. Skandan, J. Colaizzi, W.E. Mayo, J. Thermal Spray Technology 9 (2000) 483-487
- [22] X. Nie, E.I. Meletis, J.C. Jiang, A. Leyland, A.L. Yerokhin, A. Matthews, Surface and Coatings Technology 149 (2002) 245-251
- [23] R.L. Twite, G.P. Bierwagen. Progress in Organic Coatings 33 (1998) 91-100
- [24] E.I. Meletis, X. Nie, F.L. Wang, J.C. Jiang, Surface & Coatings Technology, 150 (2002), 246-256.
- [25] X. Nie, C. Tsotsos, A. Wilson, A.L. Yerokhin, A. Leyland, A. Matthews, Surface & Coatings Technology, 139 (2001), 135-142.

- [26] A.A. Voevodin, A.L. Yerokhin, V.V Lyubimov, M.S. Donley, J.S. Zabinski, *Surface & Coatings Technology*, 86-87 (1996), 516-521.
- [27] X. Nie, E.I. Meletis, J.C. Jiang, A. Leyland, A.L. Yerokhin, A. Mathews, *Surface & Coatings Technology*, 149 (2002), 245-251.
- [28] L.Rama Krishna, K.R.C. Somaraju, G. Sundararajan, *Surface & Coatings Technology*, 163-164 (2003), 484-490.
- [29] G. Sundararajan, L. Rama Krishna, *Surface & Coatings Technology*, 167 (2003), 269-277.
- [30] X. Nie, A. Wilson, A. Leyland, A. Matthews, *Surface & Coatings Technology*, 131 (2000), 506-513.
- [31] X. Nie, A. Leyland, A. Matthews, *Surface & Coatings Technology*, 125 (2000), 407-414.
- [32] G. Sundararajan, L. Rama Krishna, *Surface & Coatings Technology*, 167 (2003), 269-277.
- [33] X. Nie, A. Wilson, A. Leyland, A. Matthews, *Surface & Coatings Technology*, 131 (2000), 506-513.
- [34] X. Nie, A. Leyland, A. Matthews, *Surface & Coatings Technology*, 125 (2000), 407-414.
- [35] A.L. Yerokhin, V.V. Lyubimov, R.V. Ashitkov, *Ceramics International*, 24 (1998), 1-6.
- [36] L.O. Snizhko, A.L. Yerokhin, A. Pikington, N.L Gurevina, D.O. Misnyankin, A. Leyland, A. Matthews, *Electrochimica Acta*, 49 (2004), 2085-2095.
- [37] Mustafa Balat. *Energy Sources*, 27(2005):569-577
- [38] P. Bergeron, *Environmental impacts of bioethanol*, *Handbook on Bioethanol: Production and Utilization*. Washington DC: Taylor & Francis, 1996
- [39] Y. Fovet, L. Pourreyron, J.-Y. Gal, *Dental Materials* 16 (2000) 364–373
- [40] M. Tavakkolizadeh,¹ H. Saadatmanesh, *Journal of Composites for construction*. August 2001, 200-209

CHAPTER 2

LITERATURE REVIEW

Plasma Electrolytic Oxidation (PEO), also called Micro-arc oxidation (MAO), is a plasma-chemical and electrochemical process. The process combines electrochemical oxidation with a high voltage spark treatment in an alkaline electrolyte, resulting in the formation of a physically protective oxide film on the metal surface to enhance wear and corrosion resistance as well as prolonging component lifetime. It is suitable for the surface oxidation and pigmentation of aluminum, titanium, niobium, zirconium, magnesium and their alloys. The treated components are used in the building, mechanical, transportation and energy sectors. The technology is simple and energy saving and offers high throughput, low cost, high film quality, wide range of color pigmentation as well as environmental friendliness.

This advanced anodizing process started to be developed by Russian scientists in the mid-1970, G.A. Markov and G.V. Markova [1, 2]. They did research on investigating wear resistant property of coatings for lightweight metals. The technology has later become to be known as ‘micro-arc-oxidation’ (MAO) process [3]. In the 1980s, ‘micro-arc’ or ‘electrical discharges’ in the oxide deposition process were attempted to apply on various metals in Russia by Snezhko [4-9], Markov [10-12], Fyedorow [13], Gordienko, [13-16] and their coworkers. In Germany early industrial applications were introduced by Kurze and coworkers [17-25]. In recent years, researchers in United Kingdom, North America and China were also involved in this field. Owing to the relatively sparse information on process phenomenology and, sometimes, a short of understanding, different (and not always physically correct) terminology has been used in much of the above studies for that is, essentially, the same technique: ‘micro-plasma oxidation’, ‘anode spark electrolysis’, ‘plasma electrolytic anode treatment’ (anode oxidation under spark

discharge), being typical examples of descriptions common to 'plasma electrolytic oxidation' (PEO).

The process can make dense, very hard - nearly as hard as corundum - tenacious coatings on aluminum and aluminum alloy surface. An important characteristic of this coating is that the hard oxide layer actually grows inward from the aluminum substrate surface. Thus, good adhesion and dimensional stability of the part is possible and the parts in the nearly finished, machined condition can be coated. Unlike other superhard coatings (PVD, CVD coatings or hard anodizing alumina coatings), the coating is compliant for thicknesses up to 100µm. Because of those attractive properties, recently the PEO coatings were investigated for automotive applications, in particular, powertrain parts.

1. The PEO equipment

Plasma electrolytic oxidation (PEO) or micro-arc oxidation (MAO) changed from the conventional anodizing process. Thus, the processing equipment for PEO is relatively similar to that for the anodizing process except for the higher voltage power source. Fig. 2.1 shows the typical treatment unit for PEO process [26]. The treatment unit consists of an electrolyser (Fig. 2.1 (b)) and a high power electrical source. The electrolyser is usually a water-cooler bath placed on a dielectric base and confined in a grounded steel frame, which has an insulated current supply and a window to observe the process in operation. A stainless steel plate is immersed in the base which serves as the counter-electrode. In some examples, the electrolyser incorporates electrolyte mixing, recycling, and gas exhausting arrangements, as well as some safety interlocks.

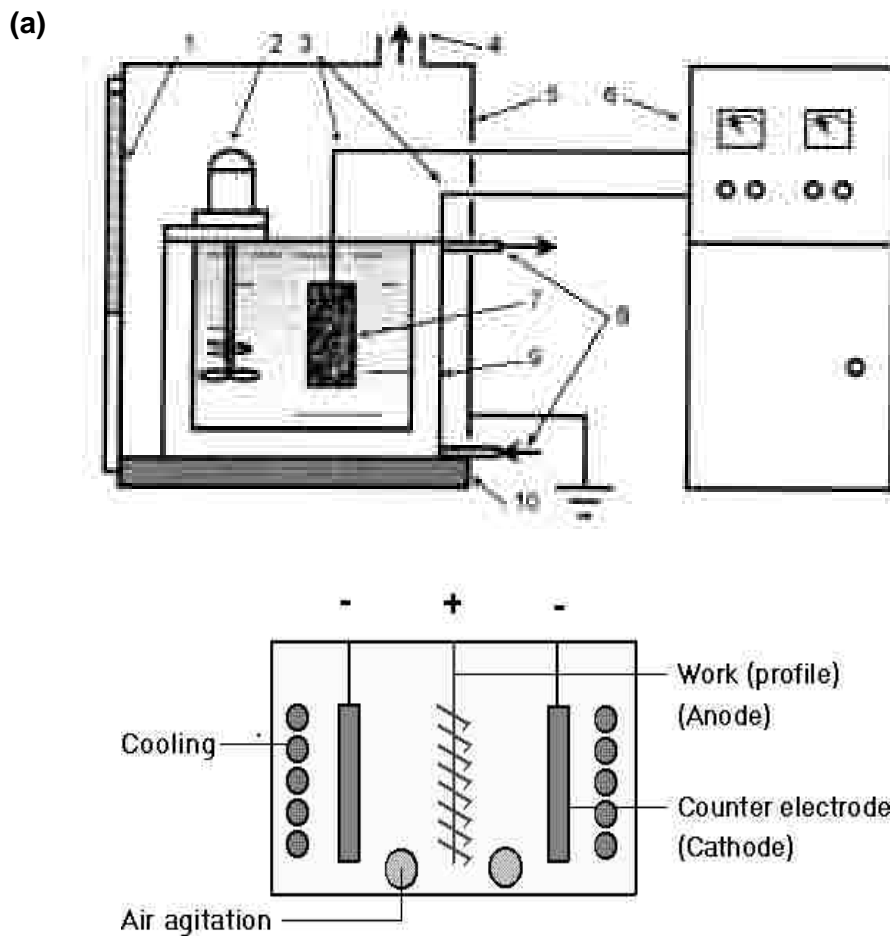


Fig. 2.1 (a) Typical arrangement of the equipment used for PEO treatment (1. window, 2. mixer, 3. connecting wires, 4. exhaust/ventilation system, 5. grounded case, 6. power supply unit, 7. workpiece, 8. cooling system, 9. bath, 10 insulating plate). (b) Electrolyte bath [26].

2. Deposition procedure

After simple pre-treatment consisting of degreasing and cleaning, samples are attached to the current supply of the unit and typically immersed in the bath at a depth of 40mm to 50mm beneath the electrolyte surface. After the electrolyte cooling, mixing and gas exhaust are activated, the working voltage can be applied to the electrolyser terminal and adjusted at the

power supply in accordance with the selected treatment regime. For the different purpose, the PEO treatment is typically carried out for between 3 and 180min at current densities of 500-2000Am⁻² and voltages of up to 800V.

Phenomena during the PEO process

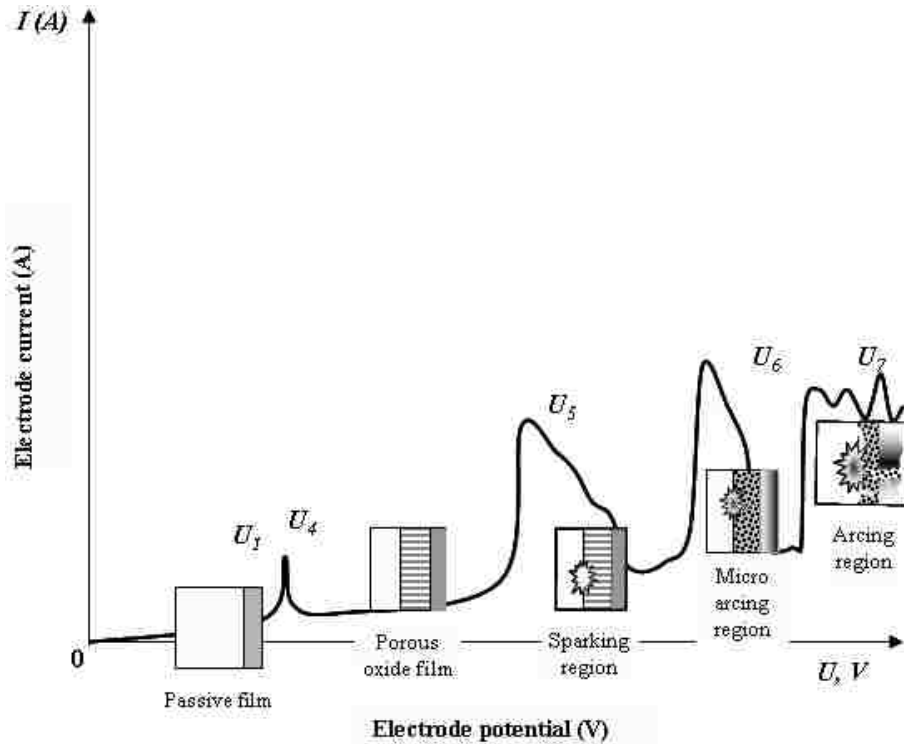


Fig. 2.2 Current-voltage diagram for the processes of plasma electrolysis: discharge phenomena are developed in the dielectric film on the electrode surface [26].

A.L. Yerokhin and X. Nie (1999) et. al. [26] discovered electrical plasma process and described the current-voltage characteristics during the PEO process. Fig. 2.2 represents the current-voltage characteristics of a system where oxide film formation occurs during the PEO process. Step 1, the passive film previously created starts to dissolve at point U_4 , which, in practice, relates to the corrosion potential of the material. Step 2, in the region of repassivation U_4 - U_5 , a porous oxide

film starts to grow, across which most of the voltage drop occurs. Step 3, at point U_5 , the electric field strength in the oxide film reaches a critical value at which the film is broken through due to impact or tunnelling ionisation. Step 4, at point U_6 , the mechanism of impact ionisation is supported by the onset of thermal ionisation processes and larger, slower arc-discharges arise. Step 5, in the region U_6 - U_7 , thermal ionisation is partially blocked by negative charge build-up in the bulk of the thickening oxide film, resulting in discharge-decay shorting of the substrate. After the point U_7 , because of negative charge blocking effects can no longer occur, the arc micro-discharges occurring throughout the film penetrate through to the substrate and transform into powerful arcs, which may cause damage effects such as thermal cracking of the film coating.

3. PEO coating structure

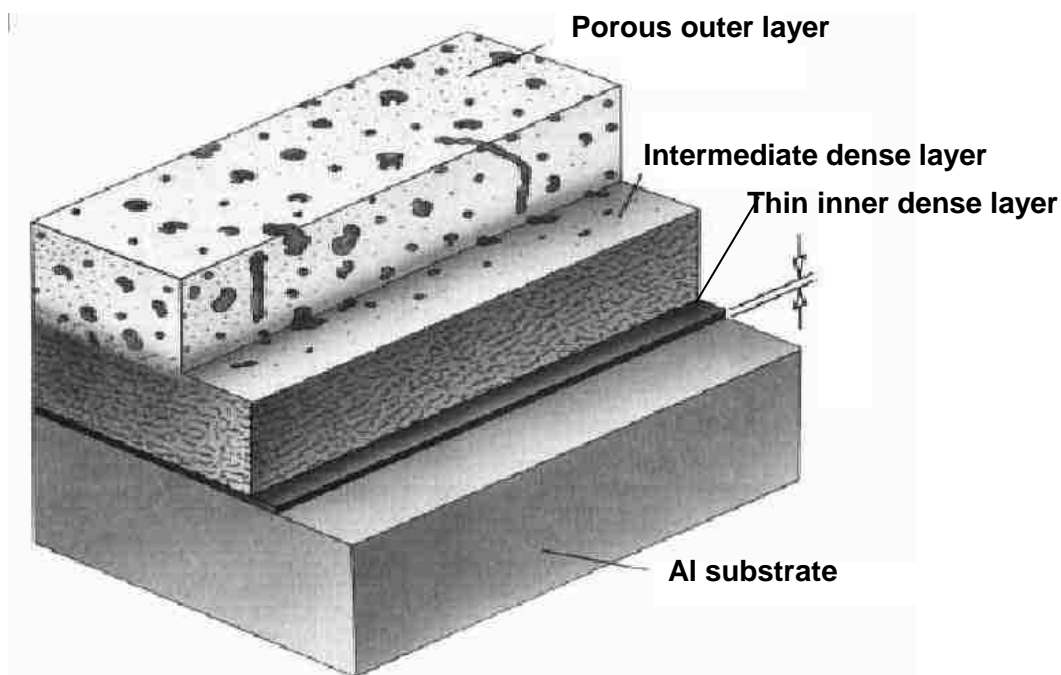


Fig. 2.3 Illustrates the structure of the PEO coating [27].

SEM investigations show that alumina coatings, produced on Al alloys by the PEO technique, have three layers, from top to bottom, a porous outer layer, intermediate dense layer and thin inner dense layer. The porous outer region consists predominantly of the low temperature modification of Al_2O_3 (γ - Al_2O_3 / η - Al_2O_3) and X-ray amorphous phases. A dense inner region is formed by mixture high temperature α , γ - Al_2O_3 modifications of Al_2O_3 and complex Al-X-O phases (X is the element from electrolytes), whereas complex phases of the substrate alloying elements are observed in a thin, interfacial region below the dense layer. The relative sizes of the regions, their structure and composition are substantially affected by substrate composition, electrolyte composition and treatment regime. Comprehensive studies of these effects have been carried out for the treatment of Al-alloys in silicate solution [28, 29]. In those researches, different current density, treatment time, and concentrations of Na_2SiO_3 (10-30g/l) with addition of 6-8g/l of KOH solution were used to produce coatings with different ratios of Al_2O_3 and SiO_2 fractions. It has been discovered that the increase of the silicon content in the electrolyte results in a higher growth rate by the formation of composite coatings and an extension of the inner dense layer. The relative proportion of the harder α -alumina is increased by raising the current density.

4. Tribological properties of PEO coatings

The PEO technology can produce superhard and thick ceramic coatings which generally have outstanding load-support characteristics. Its tribological applications have attracted much attention. Several studies have been reported on the tribological properties of the PEO coatings.

X. Nie [30] reported the effect of coating thickness on the tribological properties. The properties of the coatings with thickness from 100 μm to 250 μm were tested using a “ball-on-plate”

reciprocating-sliding test with a load of 10N over 5000 cycles, at a frequency of 2Hz. The length of sliding path was 10mm with temperature and humidity controlled to 25 ± 1 °C and $45 \pm 5\%$. The friction coefficients (c.o.f) of the PEO coating against bearing steel (BS) and tungsten carbide (WC) balls lay in the ranges 0.64-0.68 and 0.68-0.86, respectively, which is higher than the steady-state values for the uncoated substrate, however those coatings all showed excellent wear resistance. The dry wear rates were in the range 10^{-8} - 10^{-9} mm³/Nm, which compares favourably with the untreated alloy substrate at $\sim 10^{-4}$ mm³/Nm. It was found that the PEO coatings of intermediate thickness (150µm) showed relatively poor wear resistance relative to their thicker and thinner counterparts. In addition, for the intermediate thickness samples the wear rate against the BS counterface was larger than that against WC. The reason could be that the wear mechanism changed from adhesive and fatigue wear to abrasive wear as well as adhesive and fatigue.

In Ref. 31, PEO were applied in SAE 6061 aluminum alloy cylinder liners of a 4.6L-V8 aluminum block engine. The coating surface was honed and material removal during honing to obtain finished bore diameter specified. Friction properties of the PEO coatings along with a production engine cast-iron liner were evaluated in a cylinder bore/piston ring test rig (Fig. 2.4) capable of testing cast iron and the PEO specimens simultaneously under low speed-maximum load engine operating condition which represents the most severe boundary friction condition that the cylinder bores are subjected to. PEO coatings showed much lower friction than the cast-iron liner, and with high density PEO coatings, lower wear result can be achieved.

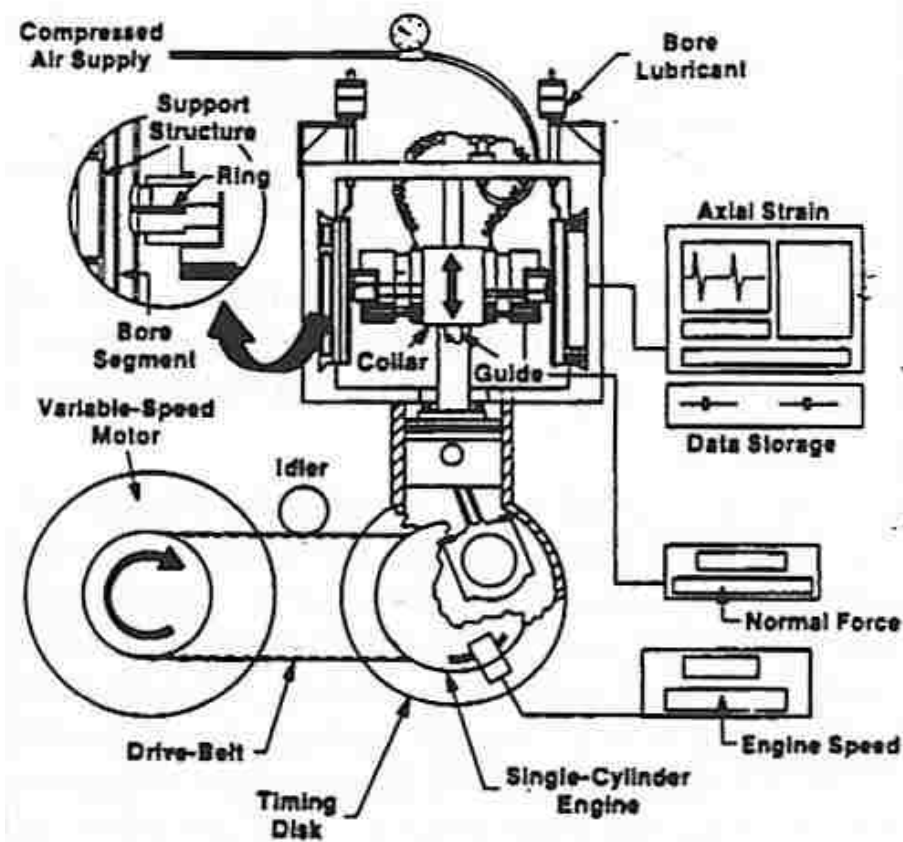


Fig. 2.4 Segmented Ring/Bore Liner test rig is an apparatus for accurate and direct comparative friction measurements between cast iron and coated bore and ring samples and oil viscosity at speeds from 100 to 600rpm [31].

Although the PEO coatings have excellent wear resistance, for sliding wear applications, such alumina coating often exhibit relatively high friction coefficients against many counterface materials. Thus, there are also many prospects for the improvement of the PEO coatings with low friction and high counterface compatibility.

5. General corrosion characteristics of Al alloys

Neutral or nearly neutral (pH from 5 to 8.5) solutions of most inorganic salts cause negligible or minor corrosion of Al alloys at room temperature. Any attack that occurs in such solutions is likely to be highly localized (pitting) with little or no general corrosion. Solutions containing chlorides are more active than other solutions. Distinctly acid or distinctly alkaline salt solutions are generally somewhat corrosive. The rate of attack depends on the specific ions present. In acid solutions, chlorides, in general, greatly stimulate attack. In alkaline solutions, silicates and chromates greatly retard attack [32, 33].

Al alloys are not appreciably corroded by distilled water even at elevated temperatures (up to 180 °C at least). Most commercial Al alloys show little or no general attack when exposed to most natural waters at temperatures up to 180 °C [34]. However, a small amount of water can drastically affect resistance to certain anhydrous organic solutions, particularly halogenated hydrocarbons. Water vapor in the air is sufficient to cause staining upon condensation, and to support SCC (spell out??) [33]. Al alloys that do not contain Cu as a major alloying constituent are resistant to unpolluted seawater. Among the wrought alloys, those of 5xxx series have the highest resistance to seawater; among the casting alloys, those of the 356.0 and 514.0 types are used extensively for marine applications. Corrosion of Al alloys in seawater is mainly of the pitting type, as would be expected from its salinity and enough dissolved oxygen as a cathodic reactant to polarize the alloys to their pitting potentials [34].

Since one of the many applications of Al alloys is in the automotive industry, as pistons, cylinder liners and valve seats, a knowledge of their corrosion behavior in the corrosive ethanol-gasoline fuel media is necessary. A group in Brazil [35] have studied the corrosion

behavior of both a Al-Si-Cu hypereutectic alloy and grey cast iron in ethanol automotive fuels. The corrosion test medium they used was pure ethanol and ethanol with small additions (1mM) of sulphuric acid and lithium chloride. The results showed that in pure ethanol and acid containing ethanol, the Al-Si-Cu alloys had a higher corrosion resistance than grey cast iron, especially in pure ethanol. However, the addition of acid to alcohol, even in small quantities, causes dissolution of the initial oxide present on the alloy surface and impeded its formation when immersed in the environment. Moreover, in environments containing chlorides, the Al-Si-Cu alloys exhibited localized corrosion characteristics.

Corrosion of Al alloys can be prevented by many different methods, including the appropriate alloy selection and system design, environment control, and the use of inhibitors and protective coatings. The latter approach has led to the development of various surface modification and coating techniques for Al alloys to enhance their corrosion resistance, such as ion implantation, sol-gel coatings, conversion coatings, CVD, PVD and thermal spraying [36-45]. Although each of these techniques possesses its own advantages, their limitations and disadvantages are also quite obvious. Most of these methods involve high temperatures during processing (CVD, PVD and thermal spray) or post-treatment (sol-gel), which may damage the coating and /or substrate [46]. In addition, sol-gel processing has been of limited use due to poor interfacial adhesion, and shrinkage and oxidation of the substrate. Ion implantation has found limited success in increasing the pitting potential of coatings. Conversion coatings are mainly based on chromium compounds that exhibit good corrosion resistance, but have also been proven to be highly toxic and carcinogenic [47, 48-53]. Since these processes have recently been reviewed, they are only briefly mentioned here [48-53]. The following subsections concentrate on a conventional surface modification technique, anodizing, together with the relatively new PEO technique.

The corrosion resistance of the PEO coatings on aluminum alloys was studied by X. Nie and coworkers [54]. Fig. 2.5 shows the polarization curves of the alumina coated alloy (with coating thickness of 250 μm) and the untreated Al alloy substrate. Both types of sample were immersed in 0.5M NaCl solution for 1h, 1day and 2 days before corrosion tests. A stainless steel AISI 316L sample was also used in the corrosion test for comparison. The poor corrosion protection property of the uncoated Al substrate resulted from the fact that the corrosion resistance considerably decreased after the thin protective oxide film on the uncoated aluminium substrate surface was broken down by the corrosion processes. The PEO-coated Al alloys possessed excellent corrosion resistance in the solution-considerably better even than the stainless steel.

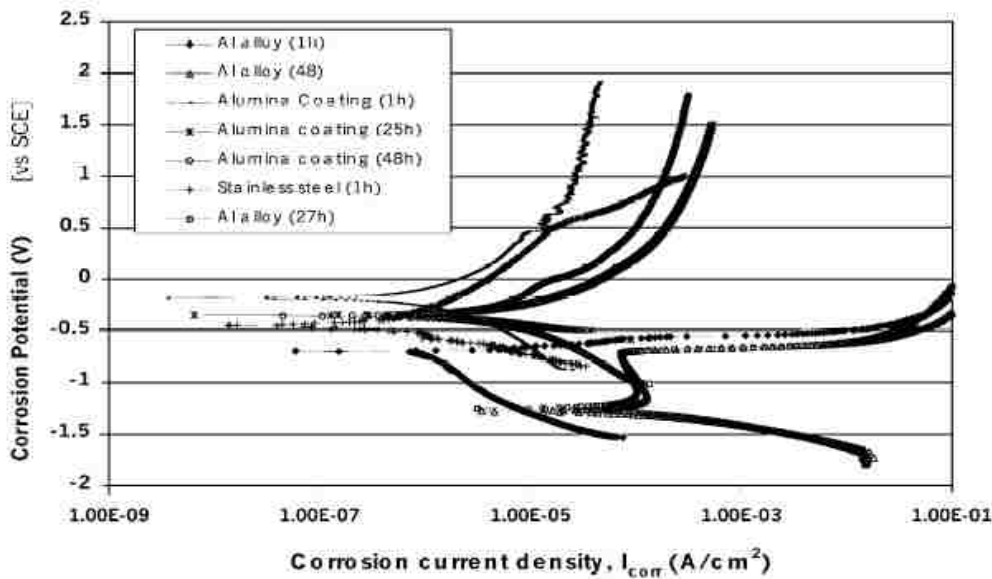


Fig. 2.5 Potentiodynamic polarization curves of untreated substrate materials and PEO alumina coatings in 0.5M NaCl solution after different immersion times [54].

6. Summary of literature review

Plasma electrolytic oxidation (PEO) of metals is a complex process combining concurrent partial processes of oxide film formation, dissolution and dielectric breakdown. The ultimate stage of the PEO treatment is a quasi-stationary stage of persistent anodic microdischarges, which exhibit a progressive change in characteristics during the electrolysis. The electrolysis is always accompanied by intensive gas evolution and localised metal evaporation due to the plasma thermochemical reactions in the microdischarges.

Four different stages of the PEO process have been identified, characterised by various formation mechanisms: (i) anodizing, (ii) anodizing film melted and broken down, (iii) micro-arc discharge and oxide coating formation, and (iv) coating composition fused and re-crystallized. The PEO coating has a three layers structure, i.e., porous outer layer, dense layer and very thin inner dense layer.

The PEO process can greatly increase hardness and corrosion resistance for Al, Mg and Ti alloys. However, there is not much research that has been done on A356 Al casting alloy for both wear and corrosion prevention in engine applications which E85 fuel or deicing salt may get involved. The PEO coating usually has high coefficient of friction. There is a need of development of a low frictional oxide composite coating. Therefore, the research in thesis was to develop PEO coatings on A356 Al alloy which would have high wear and corrosion resistance and low friction potentially for engine applications.

References

- [1] G.A. Markov and G.V. Mmarkova, USSR Patent 526961, Bulletin of Inventions, 32 (1976), 1
- [2] A.V. Nikolaev, G.A. Markov, B.I. Peshchevitskij, Izv. SO AN SSSR. Ser. Khim. Nauk, 5 (12) (1977), 32.
- [3] G.A. Markov, V.V. Tatarchuk, M.K. Mironova, Izv. SO AN SSSR. Ser. Khim. Nauk, 3 (7) (1983), 34.
- [4] L.A. Snezhko, L.A. Beskrovnyj, Yu.M. Nevkrytyj, V.I. Tchernenko, Zashch. Met., 16 (3) (1980), 365.
- [5] L.A. Snezhko, G.V. Rozenboym, V.I. Tchernenko, Zashch. Met., 17 (5) (1981), 618.
- [6] L.A. Snezhko, V.I. Tchernenko, Elektron. Obrab. Mater., (2) (1983), 25.
- [7] L.A. Snezhko, V.I. Tchernenko, Elektron. Obrab. Mater., (4) (1983), 38.
- [8] V.I. Tchernenko, L.A. Snezhko, C.B. Tchernova, Zashch., Met. 20 (3) (1984), 454.
- [9] L.A. Snezhko, S.G. Pavlus, V.I. Tchernenko, Zashch. Met., 20 (4) (1984), 292.
- [10] G.A. Markov, M.K. Mironova, O.G. Potapova, Izv. AN SSSR. Ser. Neorgan. Mater., 19 (7) (1983), 1110
- [11] A.A. Petrosyants, V.N. Malyshev, V.A. Fyedorov, G.A. Markov, Trenie Iznos, 5 (2) (1984), 350.
- [12] V.N. Malyshev, S.I. Bulychev, G.A. Markov, V.A. Fyedorov, A.A. Petrosyants, V.V. Kudinov, M.H. Shorshorov, Fiz. Khim. Obrab. Mater., (1) (1985), 82.
- [13] V.A. Fyedorov, V.V. Belozarov, N.D. Velikosel'skaya, S.I. Bulychev, Fiz. Khim. Obrab. Materialov, 4 (1988), 92.
- [14] V.S. Rudnev, P.S. Gordienko, preprint no. 3384-B87, Inst. Khimii DVO AN SSSR, Vladivostok, 1987.

- [15] O.A. Khrisanfova, P.S. Gordienko, preprint no. 2986-B89, Inst. Khimii DVO AN SSSR, Vladivostok, 1987.
- [16] P.S. Gordienko, P.M. Nedorozov, L.M. Volkova, T.P. Yarovaya, O.A Khrisanfova, *Zashch. Met.*, 25 (1) (1989), 125.
- [17] P. Kurze, W. Krysmann, G. Marx, *Z. Wiss, Tech. Hochsch. Karl-Marx-Stadt*, 24 (1982), 139.
- [18] K.H. Dittrich, W. Krysmann, P. Kurze, H.G. Schneider, *Cryst. Technol.*, 19 (1) (1984), 93.
- [19] W. Krysmann, P. Kurze, K.H. Dittrich, H.G. Schneider, *Cryst. Technol.*, 19 (7) (1984), 973.
- [20] P. Kurze, J. Schreckenbach, T. Schwarz, W. Krysmann, *Metalloberflaeche*, 40 (12) (1986), 539.
- [21] L.S. Saakian, A.P. Yefremov, L.Y. Ropyak, A.V. Apelfeld, *CorrosionControl and Environment Protection. Informative survey*, VNIOENG, Moscow, (6), 1986.
- [22] V.A. Fyedorov, A.G. Kan. R.P. Maksutov, *Surface Strengthening of Oil & Gas Trade Facilities by Micro Arc Oxidation*, VNIOENG, Moscow, (6) 1989.
- [23] G.A. Markov, B.S. Gizatullin, I.B. Rychazhkova, USSR Patent 926083, *Bulletin of Inventions*, 17, 1982.
- [24] L.A. Snezhko, V.I. Techernenko, USSR Patent 973 583, *Bulletin of Inventions* 23, 1982.
- [25] P. Kurze, W. Krysmann, G. Marx, K.H. Dittrich, DDR Patent DD-WP C25 D/236988(5).
- [26] A.L. Yerokhin, X. Nie, A. Leyland, A. Matthews, S.J. Dowey, *Surface & Coatings Technology*, 122 (1999), 73-93
- [27] www.techplate.com.tw, supported by Techplate International Co., Ltd.
- [28] A.A. Voevodin, A.L. Yerokhin, V.V Lyubimov, M.S. Donley, J.S. Zabinski, *Surface & Coatings Technology*, 86-87 (1996), 516-521.

- [29] A.L. Yerokhin, A.A. Voevodin, V.V. Lyubimov, J. Zabinski, M. Donley, *Surface & Coatings Technology*, 110 (1998), 140-146.
- [30] X. Nie, A. Leyland, H.W. Song, A.L. Yerokhin, S.J. Dowey, A. Matthews, *Surface and Coatings Technology*, 116-119 (1999), 1055-1060
- [31] V.D.N Rao, H.A. Cikanek, B.A. Boyer, SAE paper, 970022, 1997
- [32] R. Winston Revie, *Uhlig's Corrosion Handbook (2nd Edition)*, John Wiley & Sons Inc, Canada, 2000.
- [33] R.Baboian, *Corrosion Tests and Standards: Application and Interpretation*. Philadelphia, PA: ASTM, 1995
- [34] R. Winston Revie, *Uhlig's Corrosion Handbook (2nd Edition)*, John Wiley & Sons Inc, Canada, 2000.
- [35] S.M. Traldi, I. Costa, J.L. Rossi, *Key Engineering Materials*, 189-191 (2001) 352-357
- [36] X. Zhang, S. Lo Russo, S. Zandolin, A. Miotello, E. Cattaruzza, P.L. Bonora, L, *Corrosion Science* 43 (2001) 85-97.
- [37] P. Preston, R. Smith, A. Buchanan, J.M. Williams, *Scripta Metallurgica et Materialia* 32 (1995) 2021-2027.
- [38] M. Sheffer, A. Groysman, D. Mandler, *Corrosion Science* 45 (2003) 2893-2904.
- [39] J. Masalski, J. Gluszek, J. Zabrzski, K. Nitsch, P. Gluszek, *Thin Solid Films* 349 (1-2) (1999) 186-190.
- [40] J. Zhao, L. Xia, A. Sehgal, D. Lu, R.L. McCreery, G.S. Frankel, *Surface and Coatings Technology* 140(2001) 51-57
- [41] C. Taschner, B. Ljungberg, V. Alfredsson, I. Endler, A. Leonhardt, *Surface and Coatings Technology* 109 (1998) 257-264.

- [42] A. Larsson, M. Halvarsson, S. Rупpi, Surface and Coatings Technology 111 (1999) 191-198
- [43] J.M. Schneider, W.D. Sproul, A.A. Voevodin, A. Matthews, Journal of Vacuum Science and Technology A- Vacuum, Surfaces, and Films Part 15 (1997) 1084-1088.
- [44] D.E. Ashenford, F. Long, W.E. Hagston, B. Lunn, A. Matthews, Surface and Coatings Technology 119 (1999) 699-704.
- [45] B.H. Kear, Z. Kalman, R.K. Sadangi, G. Skandan, J. Colaizzi, W.E. Mayo, J. Thermal Spray Technology 9 (2000) 483-487
- [46] X. Nie, E.I. Meletis, J.C. Jiang, A. Leyland, A.L. Yerokhin, A. Matthews, Surface and Coatings Technology 149 (2002) 245-251
- [47] R.L. Twite, G.P. Bierwagen. Progress in Organic Coatings 33 (1998) 91-100
- [48] W.A. Badawy, F.M. Al-Kharafi, Corrosion Science. 39(1997) 681-700. 123
- [49] A.Y. El-Etre, Corrosion Science 43 (2000) 1031-1039.
- [50] S. Pyun, S. Moon, Journal of Solid State Electrochemistry 3 (1999) 331-336.
- [51] C.M.A. Brett, I.A.R. Gomes, J.P.S. Martins, Journal of the Electrochemical Society 24 (1994) 1158-1163.
- [52] B. Shaw, E. Sikora, K.Kennedy, P. Miller, E. Principe, Advances in Coatings Technologies for Surface Engineering. Proceedings of a Symposium held at the Annual Meeting of The Minerals, Metals and Materials Society, 1996,287-304
- [53] R.L. Twite, G.P. Bierwagen, Progress in Organic Coatings 33 (1998) 91-100.
- [54] X. Nie, E.I. Meletis, J.C. Jiang, A. Leyland, A.L. Yerokhin, A. Mathews, Surface & Coatings Technology, 149 (2002), 245-251.

Chapter 3

EXPERIMENTAL PROCEDURES

1. Pin-on-disc/reciprocating tribological test

The wear tests were carried out on PEO coatings, A356 Ingot substrate and oxide coating by use of a Sciland Pin/Disc Tribometer PCD-300A (see Fig. 3.1) at room temperature. Only one mode was used: reciprocating mode (sliding speed: 0.08 m/s) for the curved samples. The tribological behavior of the coatings under dry and lubrication conditions were studied at a normal load of 15N against an steel pin (AISI 52100, hardness HRC 59-60). A 1000m sliding



Fig. 3.1 Sliding tribotester attached on (a) Sciland Pin/Disc Tribometer PCD-300A (b) load cell and cantilever beam, (c) sample holder for reciprocating mode (d) sample holder plus load

distance was used for all PEO coatings. The same test conditions were used for the engine block coating but the test was used at oil condition (5W20). However, only a 250m sliding distance was used for the coating and substrate under the dry condition, and its surface profile was measured across the wear track to study its width and depth.

2. Potentiodynamic polarization testing

Potentiodynamic polarization is a technique where the potential of the electrode is monitored at a selected rate by application of a current through the electrolyte. By using the DC polarization technique, information on the corrosion rate, pitting susceptibility, passivity, as well as the cathodic behavior of an electrochemical system may be obtained.

In a potentiodynamic experiment, the driving force such as the potential voltage for anodic or cathodic reactions is controlled, and the net change in the reaction rate such as current is observed. The potentiostat (SP-150, Bio-logic brand instrument used for this research) measures the current which must be applied to the system for achieving the desired increase in driving force, known as the applied current. As a result, at the open circuit potential the measured or applied current should be zero. [1, 2]

A typical schematic anodic polarization curve is shown in figure 3.2. The scan starts from point 1 and progresses in the positive (potential) direction until termination at point 2. The open circuit potential is located at point A. At this point, the sum of the cathodic and anodic reaction rates on the electrode surface is zero. The active region is the region B where metal oxidation is the dominant reaction at this area. Point C is the passivation potential, and after the applied potential increases above this value the current density decrease with increasing potential (region D), until a passive, low current density is achieved (passive region - region E). When the potential

reached a sufficiently positive value (point F, also called as breakaway potential) the applied current rapidly increases (region G). This increase is depending on the alloy/environment combination. For some systems such as aluminum alloys in salt water this sudden increase in current cause the pitting corrosion. [1-3]

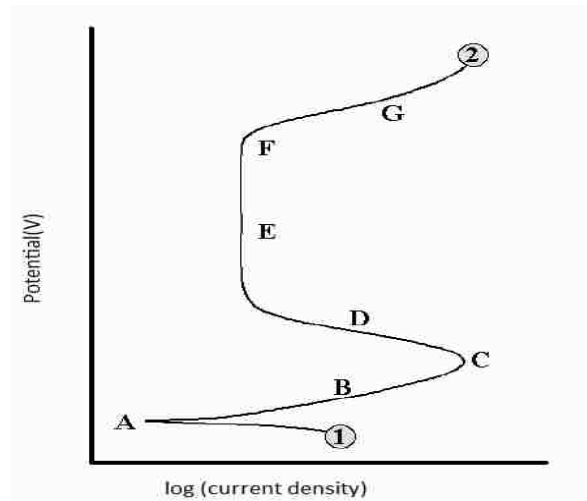


Figure 3.2 Typical polarization curve [1].

A schematic cathodic polarization scan is shown in Figure 3.3. In a cathodic potentiodynamic scan, the potential is changed from point 1 in the negative direction to point 2. The open circuit potential is located at point A. Region B represents the oxygen reduction reaction which depending on the pH and dissolved oxygen concentration in the solution. Because this reaction is limited by how fast oxygen may diffuse in solution there will be an upper limit on the rate of this reaction which is called limiting current density. Further decrease in the applied potential result in no change in the reaction rate which causes the measured current remains the same (region C). Eventually, the applied potential becomes sufficiently negative for another cathodic reaction to become operative as illustrated at point D. As the potential and driving force becomes increasingly large, this reaction may become dominant, as illustrated in

region E. This additional reaction is typically the reduction of other species in the environment such as the hydrogen evolution reaction which called the water reduction reaction. [1]

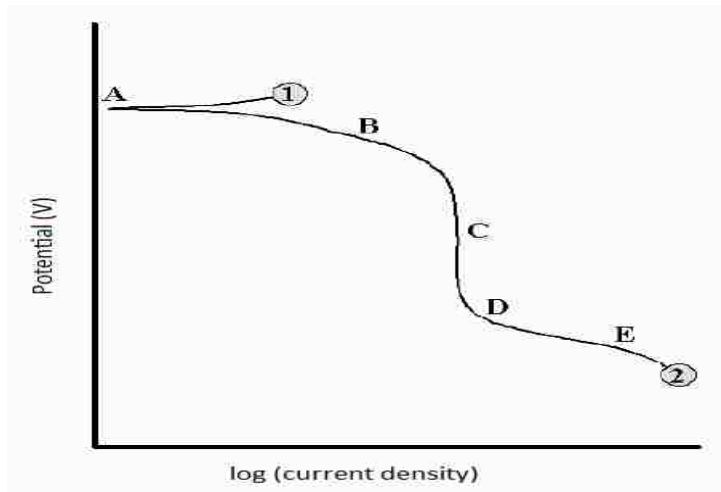


Figure 3.3 Theoretical cathodic polarization scan. [1]

For reactions which are essentially activation controlled, the current density can be expressed as a function of the overpotential, η , which is expressed in equation [3]

$$\eta = \beta \log \frac{i}{i_0} \tag{Eq.3.1}$$

Equation (3.1) is known as the Tafel equation, where β is the Tafel slope, i is the applied current density, and i_0 is the exchange current density.

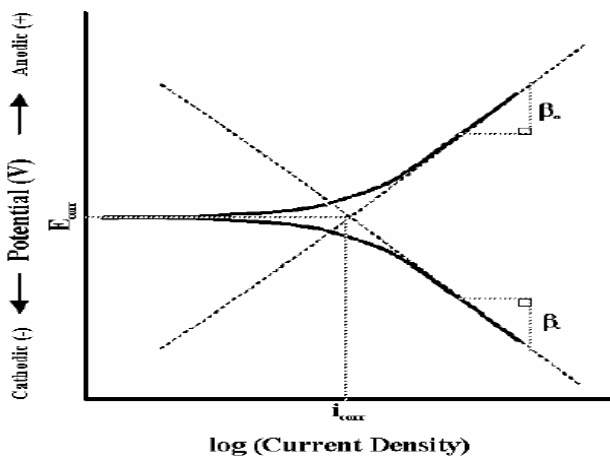


Figure 3.4 Tafel slope calculation.[3]

3. Zero Resistance Ammetry

A zero resistance ammeter is a current to voltage converter that produces a voltage output proportional to the current flowing between its two input terminals while imposing a 'zero' voltage drop to the external circuit. By using this electrochemical technique, galvanic currents between dissimilar electrode materials are measured with a zero resistance ammeter. This technique can be used to nominally identical electrodes in order to find changes occurring in the corrosive environment and thus act as an indicator of changing corrosion rates.[2]

The main principle of the technique is that differences in the electrochemical behavior of two electrodes exposed to a process stream give rise to differences in the redox potential at these electrodes. When the two electrodes are externally electrically connected, the more noble electrode becomes predominantly cathodic, then the more active electrode becomes predominantly anodic and sacrificial. After the anodic reaction is relatively stable the galvanic current monitors the response of the cathodic reaction to the process stream conditions. When the cathodic reaction is stable, it monitors the response of the anodic reaction to process fluctuations. [2]

Measurements of galvanic currents between silver and platinum coupled metals are based on the use of zero resistance amperometry (ZRA). A potentiostat controlled with a software were setup as a ZRA. The working electrode wire and the reference electrode wire combined to one served as working electrode. The counter electrode wire was not used. The ground wire connected to pure platinum served as working electrode.

Pictures in Fig. 3.5 show a setup of electrochemical corrosion test instrument.

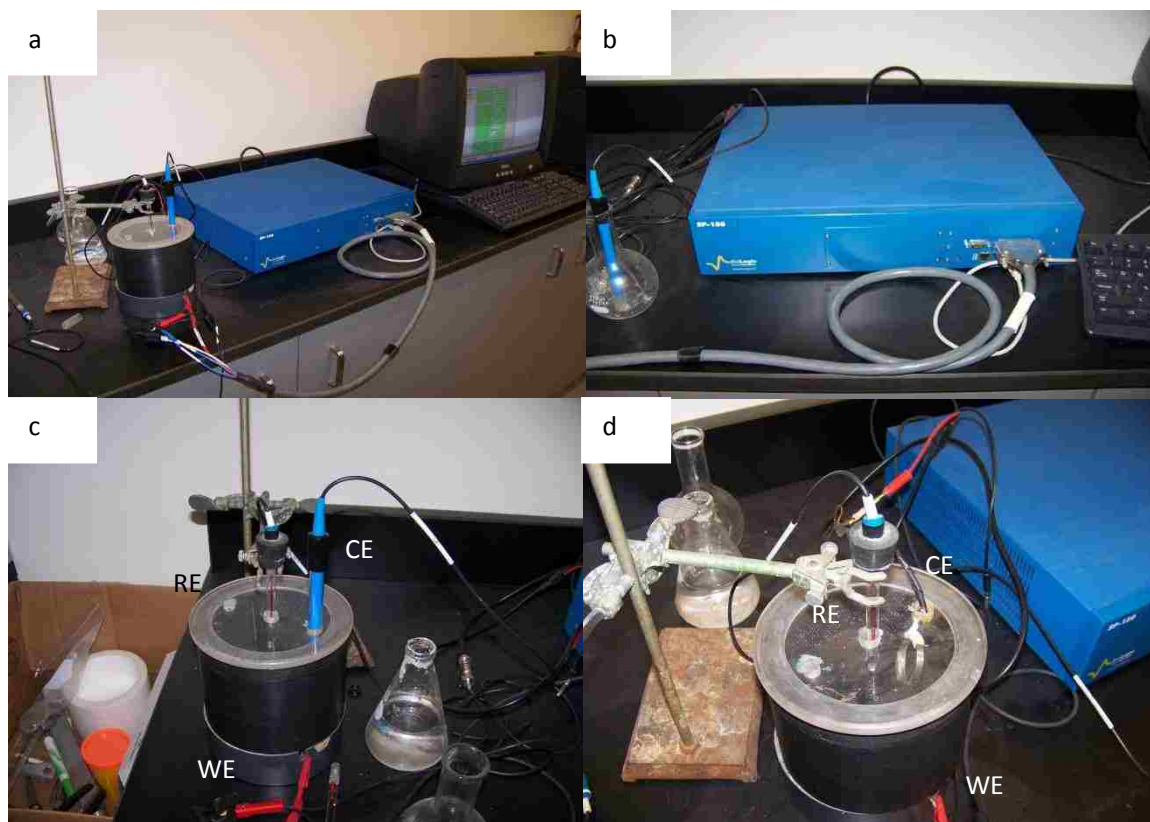


Fig. 3.5 (a, b) View of three-electrode cell and electrochemical corrosion testing equipment. (c) General galvanic corrosion test and (d) ZRA test cells arrangements.
 RE : reference electrode; WE: working electrode CE: counter electrode

References

- [1] Mythili Koteeswaran, CO₂ and H₂S Corrosion in Oil Pipelines Master Thesis of University of Stavanger June 2010
- [2] Pierre R. Roberge Chapter 4. Corrosion Inspection and Monitoring Copyright @ 2007 by John Wiley & Sons, Inc.
- [3] Denny A. Jones, Principles and Prevention of Corrosion, 2nd Edition, 1996, Prentice Hall, Upper Saddle River, NJ.

CHAPTER 4

CORROSION PROPERTIES OF PLASMA ELECTROLYTIC OXIDATION CERAMIC COATINGS ON AN A356 ALLOY TESTED IN AN ETHANOL-GASOLINE FUEL (E85) MEDIUM

1. INTRODUCTION

Government organizations and automotive manufactures have been trying to find alternative fuels to substitute for gasoline and diesel fuels because of low accessibility of energy resources and environmental issues. Ethanol which acts as a bio-based energy resource and renewable chemical can reduce both crude oil consumption and the effect of environmental pollution. The use of ethanol blended gasoline as an alternative fuel has recently shown promising results in several countries [1, 2]. The problem of ethanol blended fuel is that associated with corrosion of the materials used in vehicles. In addition, the corrosiveness of the fuel depends on the content and kind of contaminations [3, 4]. Water is expected to be present as a contaminant in small amounts in commercial fuels such as ethanol-gasoline [5, 6] and could cause the corrosion problems to the materials which come into contact with. When dissimilar materials are involved, the galvanic corrosion becomes even more problematic. Aluminium (Al) casting alloys have widely been used in automotive engine heads and cylinder blocks where a number of Al and steel couplings exist. To protect the Al from corrosion, a PEO coating technique has been used, which operates at potentials above the breakdown voltage of an oxide film growing on the surface of a passivated metal anode (i.e. Al in this case) and is characterized by multiple arcs moving rapidly over the treated surface. Complex compounds can be synthesized inside the high voltage breakthrough channels formed across the growing oxide layer. Plasma thermochemical interactions in the multiple surface discharges result in a coating growing in both directions from

the substrate surface. At a particular combination of electrolyte composition and current regime the discharge modifies the microstructure and phase composition of the substrate from a metallic alloy to a complex ceramic oxide. As a result, an oxide coating with excellent adhesion can be achieved on aluminium alloy components [7, 8].

In this study, PEO oxide coatings were prepared under different current modes. Potentiodynamic polarization and Zero Resistance Ammetry (ZRA) [9] corrosion testing methods were used to evaluate the corrosion properties of coated and uncoated Al alloys (A356) in an alternative fuel. Effects of the current modes on the coating morphologies and anti-corrosion performance were particularly discussed in this paper.

2. Experimental Details

Circular coupons (20×20×5mm) cut from an A356 alloy were ground and polished before washing in water and then drying in air. The composition of the alloy is 0.25 Cu max, 0.20 to 0.45Mg, 0.35 Mn max , 6.5 to 7.5 Si, 0.6 Fe max, 0.35 Zn max, 0.20 Ti max, 0.05 other (each) max, 0.15 others(total) max, bal Al. A PEO coating preparation system as described in Ref. [10] was used to produce the oxide ceramic coating on the coupon samples. The coatings were prepared in an alkaline electrolyte (KHPO₄, 12g/l) using different current modes [11]. Four coating samples were prepared: Sample A was coated by using unipolar current mode for 10 minutes, Sample B by using bipolar current mode for 10 minutes, Sample C by using combined unipolar (for 5 min) and bipolar (for 5 min) current mode for 10 minutes in total, and Sample D by switching the sequence for unipolar and bipolar compared with Sample C. All samples were treated under the same current density 500A/m².

Potentiodynamic polarization corrosion tests were conducted on the coatings as well as on the

uncoated A356 alloy and a steel (SAE 52100) in an ethanol (85%)-gasoline(15%) alternative fuel medium (i.e., E85). ZRA corrosion tests were also conducted to simulate galvanic corrosion between the steel and the coated/uncoated Al alloys. Scanning electron microscopy (SEM) was used to observe morphologies of the coupons before and after the tests.

3. Results

Fig.4. 1 shows the cross-sectional SEM micrographs of the sample A-D coatings. The thickness of the coatings was in the range of 4-7 μm . The coatings A and C were slightly thicker than the coatings B and D. The thinner coatings might be due to the bipolar current mode where negative currents were involved and would reduce the efficiency of coating growth. Such an effect seems more obvious when the coating process started with a bipolar mode. When the duplex treatments by combination of unipolar and bipolar current modes were used, the interfaces between coatings and substrates became less distinguishable, indicating a denser inner layer or thicker diffusion layer in coatings C and D.

Fig.4. 2 shows the potentiodynamic polarization curves for coatings A-D and uncoated A356 as well as steel in the E85 medium. The corrosion potential (E_{corr}), current density (i_{corr}) and polarization resistance (R_p) obtained by Tafel calculations for uncoated and coated samples are given in Table 1.

The (R_p) values were calculated using the relationship [12, 13]:

$$R_p = \frac{\beta_a \times \beta_c}{2.3 I_{\text{corr}} \times (\beta_a + \beta_c)} \quad \text{Eq.4.1}$$

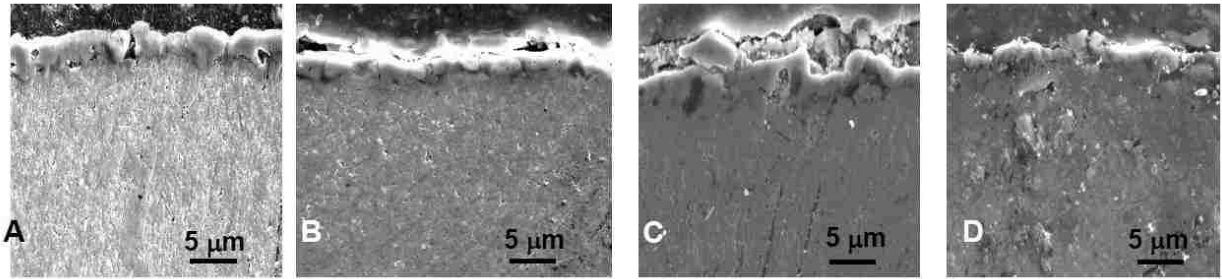


Fig. 4.1 Crossion sectional SEM micrographs of sample A-D coatings.

The corrosion resistance in the E85 medium increased in the order of steel < sample B < A356 < sample A < sample D < sample C. Compared with the uncoated A356 coupon, coated simples C and D exhibited a higher polarization resistance, a lower corrosion current density and a higher corrosion potential. Sample C with thickness 6-7 μm appeared to have the best corrosion properties among the coated A356 coupons.

Table4.1 Potentiodynamic polarization parameters of uncoated/coated A356 and steel in E85.

	β_a (mV/dec)	β_c (mV/dec)	E_{corr} (mV)	i_{corr} (μAcm^{-2})	R_p (Ωcm^2)
A356	196	223.8	-491.171	0.010	4543.04
Steel	537.0	142.3	-89.865	0.050	978.18
Sample A	314.8	239.9	-664.87	0.007	8456.31
Sample B	101.5	478.2	-612.17	0.011	3309.42
Sample C	116.3	170.6	-431.388	0.003	10022.57
Sample D	221.9	286.3	-433.272	0.006	9058.68

Fig.4.3 depicts the galvanic corrosion current density vs. time curves of studied couples: the steel and uncoated or coated A356 samples. The plots presents that the corrosion current tremendously decreased when the A356 samples had been coated with PEO oxide coatings. The positive current density values registered in the Figure indicated that those coated and uncoated A356 acted as the anodic member of the pairs (i.e., steel vs. each of the tested samples); therefore, the steel remains protected [14, 15], unlike the highest corrosion current (i.e., corrosion rate) shown

in the potentiodynamic polarization corrosion tests.

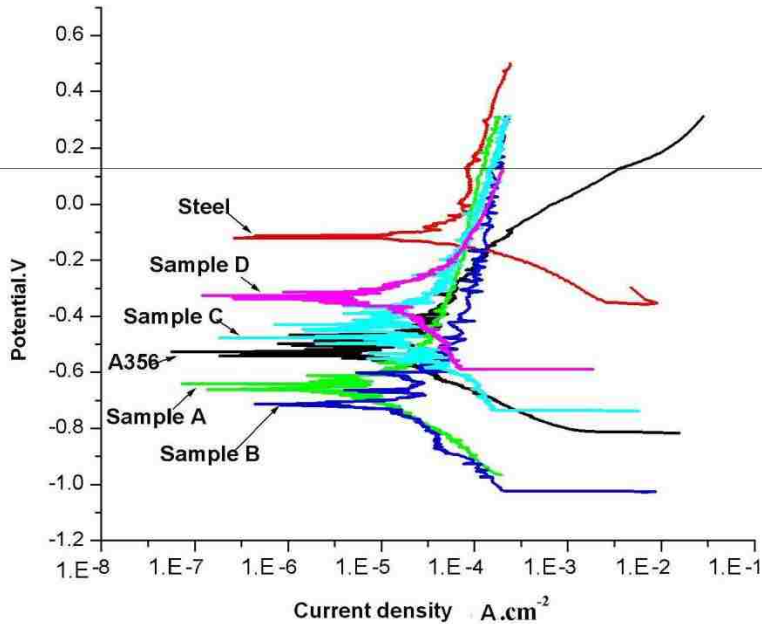


Fig. 4.2 Potentiodynamic polarization corrosion curves of the samples in an E85 medium.

A general tendency for the galvanic current density to decrease with time was observed for all coated samples. For sample A, the current density decreased during the first 11000 seconds, and then it stabilized at around $0.025 \mu\text{A}/\text{cm}^2$. The sample B had a situation similar to sample A but started with a lower current, and it decreased not as sharp as Sample A. Samples D and C showed a slight increase in the anodic current density during the first 12000 seconds then became stable and finally reached 0.005 and $0.008 \mu\text{A}/\text{cm}^2$ at the end of the test. In general, Samples C and D both showed a lower current density than Samples A and B. The reason for that could be the thicker dense inner layers for samples C and D which made the corrosion voltages (E_{corr} in Table 4 .1) closer to E_{corr} of the steel and provided a better insulator between

the corrosion medium and Al substrates. Thus, the ZRA test results also suggested that the coatings C and D had the best anti-corrosion performances, similar to the results obtained using potentiodynamic polarization corrosion tests.

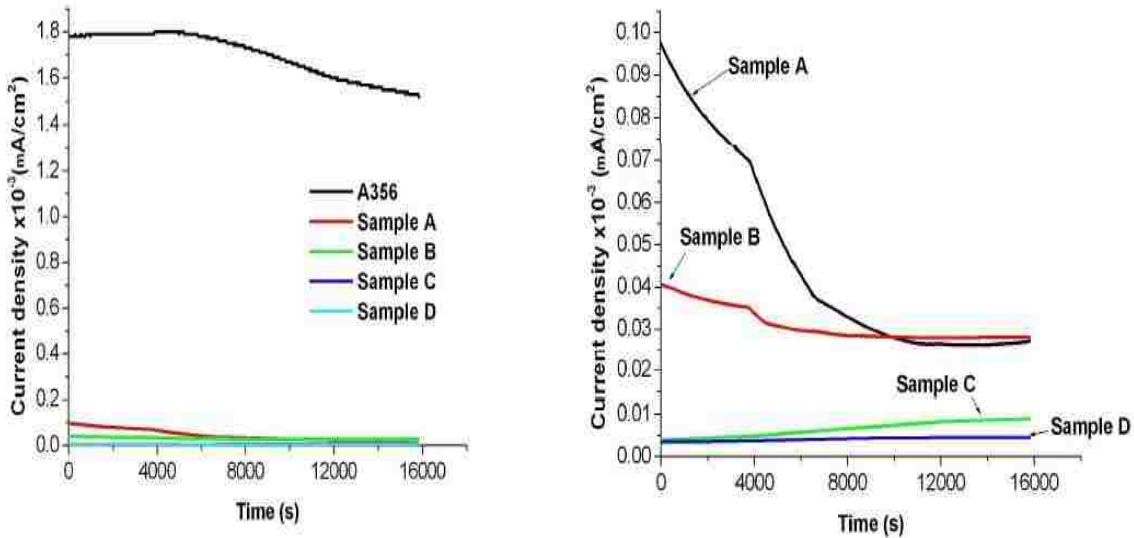


Fig. 4.3 The galvanic corrosion current density of the test samples in the E85 medium

Fig. 4.4 is the SEM micrographs of the surface morphologies of the tested materials after ZRA corrosion tests in E85. Apparently, all the samples suffered corrosion to different degrees. The uncoated A356 sample was experienced not only a general corrosion which left scattered circular staining on the surface (Fig. 4a) but also a localized corrosion (Fig. 4b) during the testing in E85 medium. There was no obvious corrosion observed on the surfaces of samples C and D as shown in Fig.4.4 (c, d).

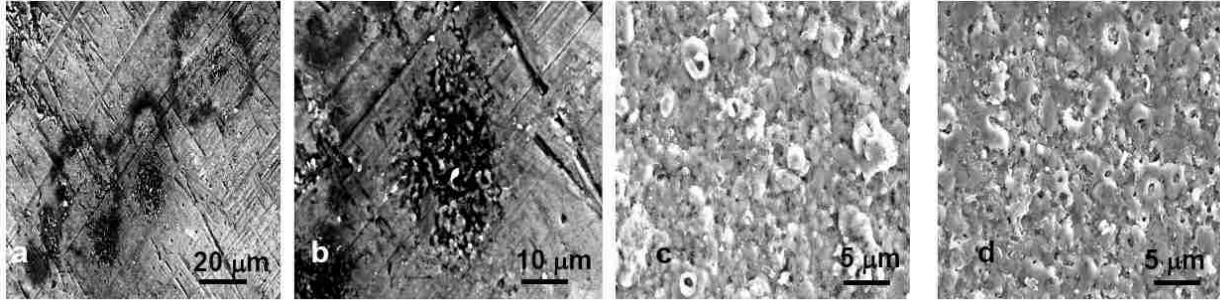


Fig. 4.4 SEM micrographs of (a, b) uncoated A356, (c) Sample C and (d) Sample D after ZRA corrosion tests.

4. Conclusions

(1) Different current modes during the PEO process were used to produce ceramic oxide coatings on an aluminium A356 substrate. The unipolar current mode would make the coating thicker than the bipolar mode. The coatings prepared using duplex unipolar and bipolar treatments had a dense inner layer or thick diffusion layer.

(2) The potentiodynamic polarization corrosion test results showed that ceramic PEO coatings significantly affected the polarization characteristics of A356 alloy. The ranking for corrosion resistance in E85 medium was sample B < A356 < sample A < sample D < sample C.

(3) Galvanic corrosion was studied under open circuit conditions using a zero-resistance ammeter (ZRA). The ZRA tests showed that in the E85 medium, coated samples all had a lower corrosion current density than uncoated A356 alloy. Samples C and D prepared using combined bipolar and unipolar current modes could perform a better galvanic corrosion resistance than other samples.

(4) Therefore, PEO ceramic coatings would provide an efficient protection to A356 alloy from the E85 corrosion.

Acknowledgement:

This research is supported by Natural Sciences and Engineering Research Council of Canada, Collaborative Research and Development Program.

References:

- [1] Identification, repair, and mitigation of cracking of steel equipment in fuel ethanol service, Technical Report No. 939-E. American Petroleum Institute. 2008.
- [2] AC Hansen, Q Zhang and PW Lyne: Ethanol–diesel fuel blends – a review, *Bioresour Technol* 96 (2005) 277–85
- [3] P Österreicher-Cunha, JRD Guimarães, Jr EDA Vargas and MIPD Silva: Study of biodegradation processes of BTEX–ethanol mixture in tropical soil, *Water Air Soil Pollut* 181 (2007) 303–17.
- [4] N Krings, J Abel, A Hebach, H Ochs, A Reitzle and S Virtanen: Corrosion in ethanol containing gasoline, In: 214th ECS Meeting. Oct 12–17; Honolulu, HI, 2008
- [5] CS Brossia, E Gileadi and RG Kelly: The electrochemistry of iron in methanolic solutions and its relation to corrosion, *Corros. Sci.* 37 (1995) 1455–71.
- [6] X Lou and PM Singh: Role of water, acetic acid and chloride on corrosion and pitting behavior of carbon steel in fuel-grade ethanol, *Corros. Sci.* 52 (2010) 2303–15
- [7] X Nie, X Li and D Northwood: Corrosion behavior of metallic materials in

ethanol–gasoline alternative Fuels, Mater Sci Forum 546-549 (2007) 1093–1100.

[8] A. L. Yerokhin, X. Nie, A. Leyland, A. Matthews and S. J. Dowey: Plasma electrolysis for surface engineering, Surf. Coat. Technol. 122 (1999) 73

[9] M.T. Montañés, R. Sánchez-Tovar, J. García-Antón and V. Pérez-Herranz: Influence of the Flowing Conditions on the Galvanic Corrosion of the Copper/AISI 304 Pair in Lithium Bromide Using a Zero-Resistance Ammeter, Int. J. Electrochem. Sci., 5 (2010) 1934 - 1947

[10] R.O. Hussein, X. Nie, D. Northwood, A.L. Yerokhin and A. Matthews: J. Phys. D Appl. Phys. 43 (2010) 105203.

[11] R.O. Hussein, X. Nie and D.O. Northwood: Influence of process parameters on electrolytic plasma discharging behaviour and aluminum oxide coating microstructure, Surf. Coat. Technol. 205 (2010) 1659–1667

[12] P. Zhang, X. Nie and D.O. Northwood: Influence of coating thickness on the galvanic corrosion properties of Mg oxide in an engine coolant, Surf. Coat. Technol. 203 (2009) 3271–3277

[13] X. Nie, E.I. Meletis, J.C. Jiang, A. Leyland, A.L. Yerokhin and A. Matthews: Surf. Coat. Technol. 149 (2002) 245-251

[14] H. Jafari, M.H. Idris, A. Ourdjini, H. Rahimi and B. Ghobadian: EIS study of corrosion behavior of metallic materials in ethanol blended gasoline containing water as a contaminant, Fuel 90 (2011) 1181-1187

[15] H.P. Hack. Corrosion: Fundamentals, Testing, and Protection, Vol 13A, ASM Handbook, ASM International, USA (2003)

CHAPTER 5

GALVANIC CORROSION PROPERTY OF CONTACTS BETWEEN CARBON FIBER CLOTH MATERIALS AND TYPICAL METAL ALLOYS IN AN AGGRESSIVE ENVIRONMENT

1. INTRODUCTION

The relationship between a vehicle's mass (weight) and its fuel economy is well known. Materials and techniques for cutting weight from vehicles are a part of routine automotive engineering practice. Large reductions in weight while maintaining size and enhancing vehicle utility, safety, performance, ride and handling are often thought of as requiring radical changes, such as the all-aluminum bodies or carbon-fiber composites sometimes featured in concept vehicles [1,2]. A carbon fiber is a long, thin strand of material about 0.005-0.010 mm diameter composed mostly of carbon atoms. The graphite basal planes oriented parallel to the axis of the fiber make the carbon fiber incredibly strong for its size. Several thousand carbon fibers are twisted together to form a yarn, which may be used by itself or woven into a fabric. The yarn of fabric is combined with epoxy and wound or molded into shape to form various composite materials. Carbon fiber-reinforced composite materials are used to make aircraft and spacecraft parts, racing car bodies, golf club shafts, bicycle frames, fishing rods, automotive springs, sailboat masts, and many other components where light weight and high strength are needed [3].

Aluminum and its alloys are widely used in a large number of industrial applications due to their excellent combination of properties, such as relatively good corrosion resistance, excellent

thermal conductivity, high strength to weight ratio, easy to deform, and high ductility. Aluminum alloys have generally been used in manufacturing automobile and aircraft components in order to make the moving vehicle lighter, which results in saving fuel consumption [4]. Aluminum is an active metal whose resistance to corrosion depends on the formation of the protective oxide film on its surface. For these reasons, a number of investigations in its electrochemical behavior and corrosion resistance have been carried out in a wide variety of media.

Carbon fibers and aluminum alloys have created considerable interest as structural engineering materials and in many applications, carbon fiber composite materials are connected to aluminum metals. When carbon fibers in a polymer based matrix composite are used as a structural component, it should be noted that carbon fiber is a very efficient cathode and very noble in the galvanic series [5-7]. Therefore, contact between carbon fiber composites and metals with similar properties in an electrolyte such as rain or seawater will be extremely undesirable. If galvanic coupling occurs, galvanic corrosion of the metal may occur. Additional possibilities of corrosion related to raising the galvanic potential, particularly for passive metals such as aluminum alloys, include: initiation of pitting corrosion and extensive crevice corrosion [8, 9].

Plasma electrolytic oxidation (PEO) coatings are much harder than anodized coatings and can be used to protect a variety of light metals (Ti, Al and Mg) and their alloys [10, 11]. The PEO process typically uses a dilute alkaline solution, which is not harmful to the environment. The coatings are typically five to a few hundred microns in thickness, with crystalline and amorphous phases containing both metal substrate and electrolyte chemical components [12, 13]. As the coating thickness increases, the PEO coating forms a porous and rough out-layer on the top of a dense layer. Depending on the current mode as well as the current pulse timing, the thickness of

the outer layer can be reduced. The improved surface performance obtained yields numerous real and potential applications for the PEO technology in the aerospace (fasteners, landing gear, blades, discs and shafts of aircraft engines), the automotive (seat frames, doors, pistons and cylinder liners), the gas and oil (gears and rotary pumps) and the biomedical industries [14, 15].

In this study, the galvanic corrosion between metals and a carbon fiber sheet were investigated. PEO oxide coatings on aluminum alloys were prepared under different current modes. In order to investigate the possibility and intensity of galvanic corrosion, not only potentiodynamic polarization test but also zero resistance ammeter (ZRA) testing methods were used to evaluate the corrosion properties of a steel and a titanium alloy as well as coated and uncoated Al alloys (A356) in 3.5% NaCl solutions. Effects of the current modes on the coating morphologies and anti-corrosion performances are extensively discussed in this paper. As a result of this study, a better understanding of the galvanic corrosion behavior of the carbon fiber-metal system can be achieved.

2. Experimental details

Circular coupons (20x20x5 mm) cut from steel ASTM A1018 an A356 alloy and a Ti6Al4V alloy were ground and polished before washed in water and then air-dried. The composition of the ASTM A1018 steel is 98.81-99.26 Fe, 0.18 C, 0.6-0.9 Mn, 0.04 max P and 0.05 max S. The composition of the A356 aluminum alloy is 0.25 Cu max, 0.20-0.45 Mg, 0.35 max Mn, 6.5-7.5 Si, 0.6 max Fe, 0.35 max Zn, 0.20 max Ti, 0.05 max others (each), 0.15 max others (total), and bal Al. The composition for Ti6Al4V is 6.0 Al, 4.0 V, 0.25 max Fe, 0.2 max O, and the remainder Ti. A PEO coating preparation system as described in Ref. [16] was used to produce the oxide ceramic coatings on the aluminum coupon samples. The coatings were prepared in an

alkaline electrolyte (KHP04, 6 g/l) plus sodium silicate powder (Na₂SiO₄, 6g/l) using different current modes [17]. For the A356 alloy, four coating samples were prepared: Sample A was coated by using the bipolar current mode with +5 positive and -2.5 mA/mm² negative current densities for 20 minutes. Sample D was coated by using the unipolar current mode (current density: +5 mA/mm², 80% duration time) for 20 minutes, Sample B by using combining unipolar (for 10 min) and bipolar (for 10 min) current modes for 20 minutes in total, and Sample C by switching the sequence of unipolar and bipolar modes used with Sample B. For Ti6Al4V samples, Sample TB was coated by using the bipolar current mode for 20 minutes and Sample TU was coated by using the unipolar mode for 20 minutes.

Potentiodynamic polarization corrosion tests (SP-150, Bio-logic®, Bandwidth: 5) were conducted on the coatings as well as on the uncoated A356 alloy, Ti6Al4V and steel ASTM A1018 in a 3.5% NaCl solution. ZRA corrosion tests [18] were also conducted to simulate galvanic corrosion between the carbon fabric and the testing samples, where the testing sample, Ag/AgCl/KCl electrode and carbon fabric (instead of Pt) were used as the working, reference, and auxiliary electrodes, respectively. During the test, galvanic corrosion was monitored under open circuit conditions using a zero-resistance ammeter for 5 minutes per cycle for 50 cycles. The total duration time was 4 hours. The probe Positector 6000 series coating thickness gauge was used for coating thickness measurement. Scanning electron microscopy (SEM) FEI Quanta 200 FEG microscope, operating at 15 kV, was used to observe morphologies of the samples before and after the tests.

3. Results and discussion

Table 5.1 shows the thickness of the aluminum coatings, determined by the probe through averaging 10 data measurements. The thickness of the coatings is in the range of 10-20 μm . The coatings of Sample A and Sample B were slightly thicker than the coatings of Sample C and Sample D. For these coating treatment cases, the thicker coatings may be due to the bipolar current mode where negative currents were involved and would enhance the efficiency of coating growth. Such an effect seemed more obvious when the coating process started with a bipolar mode. When the duplex treatments by combination of unipolar and bipolar current modes were used, the interfaces between coatings and substrates became less distinguishable, indicating a denser inner layer or thicker diffusion layer in coatings of Sample A and Sample B [19, 20].

	Coating thickness (μm)	β_a (mV/dec)	β_c (mV/dec)	E_{corr} (mV)	I_{corr} (μAcm^{-2})	R_p ($\text{k}\Omega \text{cm}^2$)
Steel	N/A	190.6	133.3	-770.0	80.0	0.43
A356	N/A	80.4	95.6	-836.5	8.0	2.37
Sample A -Bipolar	21.8	342.4	221.1	-942.1	0.8	77.88
Sample B - Unipolar/ Bipolar	17.5	150.0	150.0	-366.9	0.4	81.52
Sample C - Bipolar/ Unipolar	15.9	958.4	164.5	-1145.6	7.0	8.69
Sample D -Unipolar	12.2	247.7	215.6	-987.5	1.0	50.12

Table 5.1 Potentiodynamic polarization parameters of uncoated/coated A356 and steel in a 3.5% NaCl solution and thickness of alumina coatings.

Fig.5.1 shows the optical images for the steel ASTM A1018 and the aluminum alloy A356 after

corrosion tests. It can be seen from the pictures that the general and pitting corrosions occurred on each sample. Fig. 5.2 shows the potentiodynamic polarization curves for coating samples A-D and uncoated A356 as well as the steel in the 3.5% NaCl solution. The corrosion potential (E_{corr}), current density (i_{corr}) and polarization resistance (R_p) obtained by Tafel calculations for uncoated and coated samples are given in Table 1. The (R_p) values were calculated using the relationship [21]:

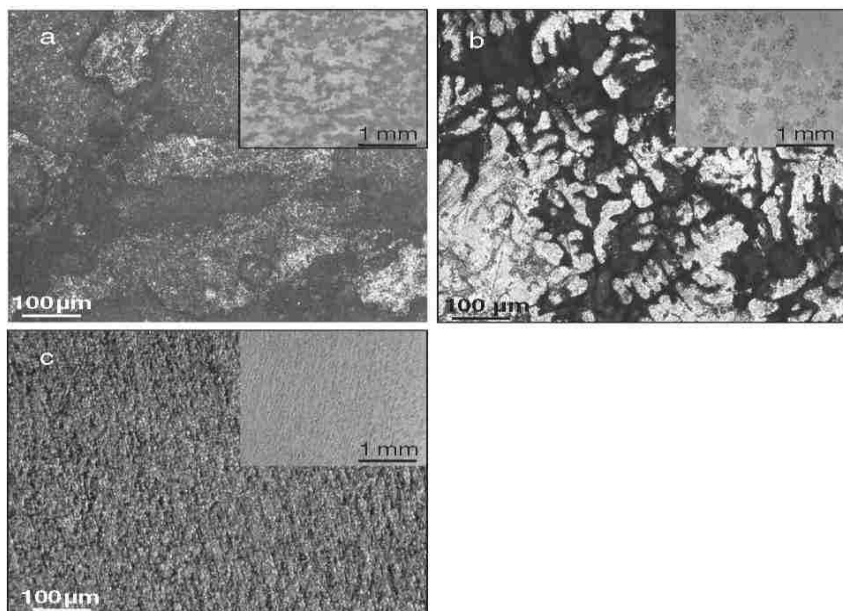


Fig. 5.1 Optical images of (a) ASTM Al018 steel and (b) aluminum alloy A356 and (c) Ti6Al4V alloys after corrosion tests in (a), (b) and (c) showed the corroded areas at a low magnification.

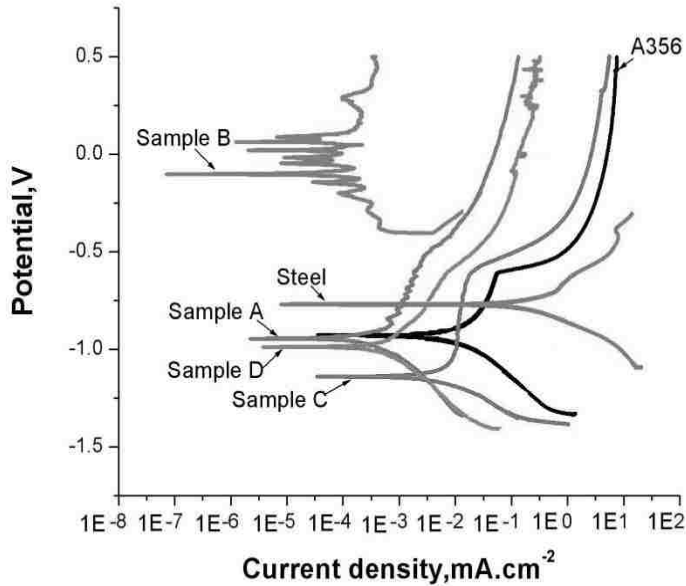


Fig. 5.2 Potentiodynamic polarization corrosion curves of the samples in a 3.5% NaCl solution. Treatment modes for samples: A- bipolar, B- unipolar/bipolar, C-bipolar/unipolar, D -unipolar.

$$R_p = \frac{\beta_a \times \beta_c}{2.3 I_{corr} \times (\beta_a + \beta_c)} \quad \text{Eq.5.1}$$

From Table 1, the steel had the highest corrosion current, even higher than uncoated aluminum A356. Samples A and D had a similar corrosion current density and corrosion resistance. Sample B, prepared by unipolar followed by bipolar current treatments, possessed the lowest corrosion current and highest corrosion resistance. However, Sample C, which was prepared by bipolar and unipolar current modes, presented a low corrosion resistance although it was better than the uncoated aluminum sample. The results indicated that the coating process greatly influenced the coating performance. The aluminum sample (Sample B), treated first using unipolar then bipolar modes, outperformed other samples. The corrosion resistance in the 3.5% NaCl solution

increased in the order of steel < A356 < Sample C < Sample D < Sample A < Sample B. Compared with the uncoated A356 coupon, coated Samples A and B exhibited a higher polarization resistance, a lower corrosion current density and a higher corrosion potential. Sample B with thickness 17.5 μm appeared to have the best corrosion properties among the coated A356 coupons.

Fig. 5.3 depicts the galvanic corrosion current density vs. time curves of studied couples: the carbon fiber and uncoated or coated A356 samples and steel. The plots present that the corrosion current tremendously decreased when the A356 samples had been coated with PEO oxide coatings. The positive current density values registered in Fig.5.3 indicated that the coated and uncoated A356 acted as the anodic member of the pairs (i.e., carbon fiber vs. each of the tested samples). Therefore, the coated aluminum remains with a tendency to be corroded, but the corrosion rate was much lower than the uncoated aluminum, unlike the very high corrosion current (i.e., corrosion rate) shown by the A356 in the potentiodynamic polarization corrosion tests.

A general tendency for the galvanic current density to decrease with time was observed for all coated samples. For Sample A, the current increased during the first 12,000 s, and then it stabilized at around 0.025 mA/cm^2 . Sample D had a situation similar to Sample A but started with a higher current, then decreased at 8000 s, which is not as sharp as Sample A, but ended at $0.08 \mu\text{A/cm}^2$. Samples B and C showed a slight smoothed curve in the anodic current density during the first 12,000 s then became stable and finally reached 0.001 and $1.1 \mu\text{A/cm}^2$ at the end of the test, respectively. In general, Samples A and B both showed a lower current density than Samples C and D. The reason for that could be the thicker dense inner layers for Samples A and B which made the corrosion voltages (E_{corr} in Table 1) closer to the corrosion voltages of the

carbon fiber and provided a better insulator between the corrosion medium and the tested samples. Thus, the ZRA test results also suggested that the coatings of Samples A and B had the best anti-corrosion performances, similar to the results obtained using potentiodynamic polarization corrosion tests.

Fig. 5.4 is the SEM micrographs of the surface morphologies of the tested materials which are the uncoated A356 and the aluminum coated A356 after ZRA corrosion tests in 3.5% NaCl solutions. Apparently, the ASTM A1018 steel sample suffered severe corrosion as shown in Fig.5.1 while the Ti sample showed no sign of corrosion. The uncoated A356 sample experienced not only a general corrosion which left scattered circular staining on the surface (Fig. 5.4a) but also a localized corrosion (Fig.5.4b) during the testing. There was no obvious corrosion observed on the surfaces of coated A356 samples as shown in Fig. 4 for Samples B (Fig.5. 4c) and C (Fig. 5.4d). Sample B in Fig. 5.4c presented a very dense coating surface with a minimum number of pores, which was attributed to the very good anticorrosion properties as shown in both potentiodynamic polarization corrosion and ZRA corrosion tests. Therefore, the coating process operation combined with first the unipolar current mode and then the bipolar current mode would provide the best coating performance for the aluminum alloy in the corrosion tests.

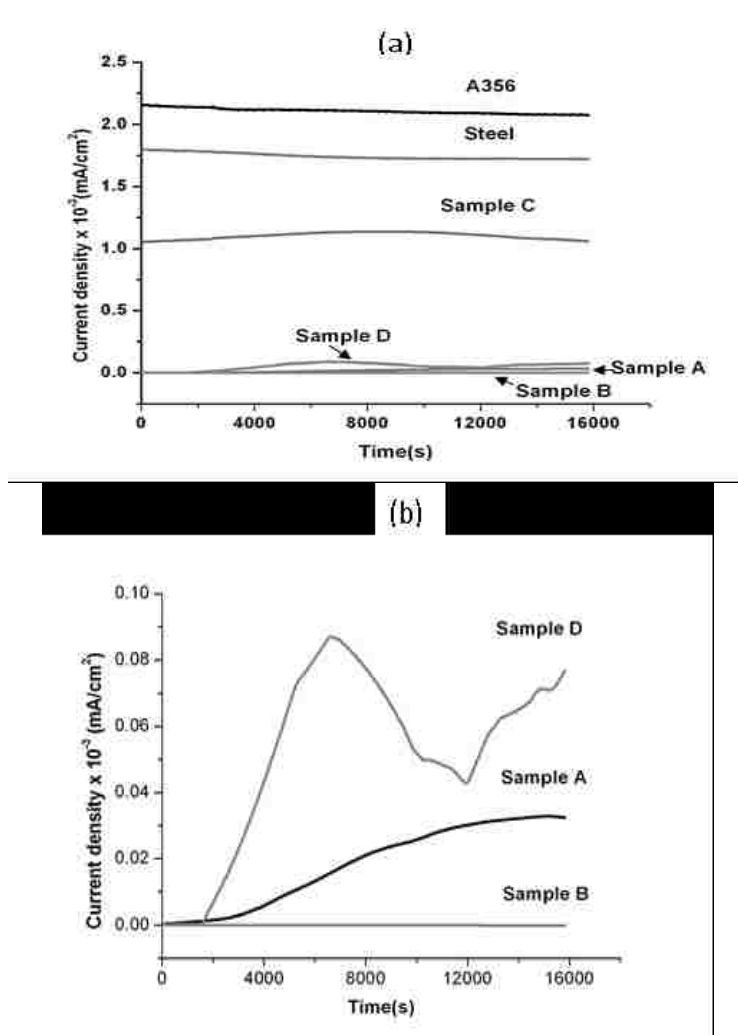


Fig.5.3. The galvanic corrosion current density curves of the test samples in the 3.5% NaCl solution for (a) all samples and (b) samples A, B and D magnified scale. A -bipolar, B - unipolar/bipolar, C - bipolar/unipolar, D - unipolar.

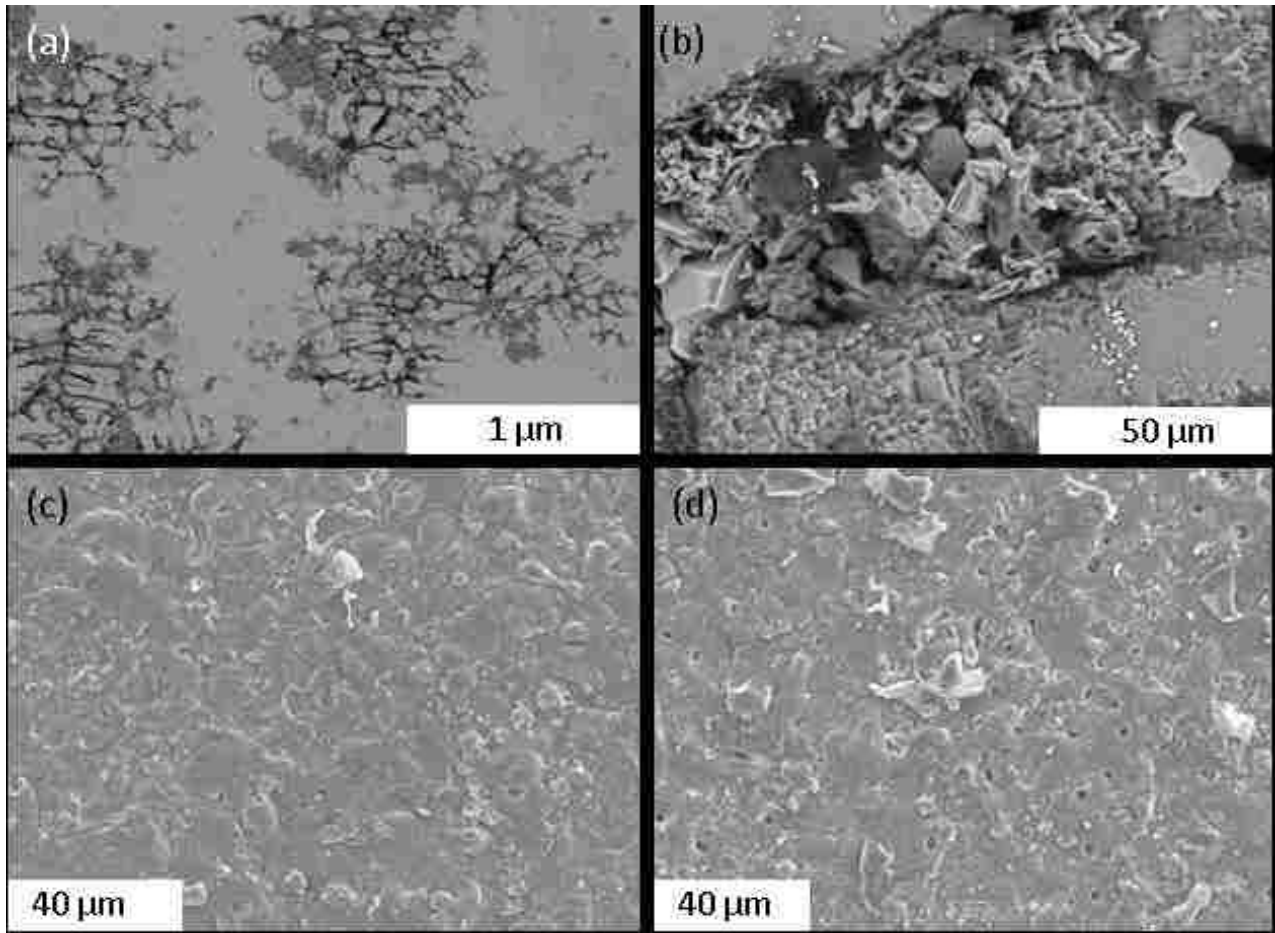


Fig. 5.4 SEM micrographs of (a, b) uncoated A356. (c) Sample Band (d) Sample C after ZRA corrosion tests.

Fig.5. 5 shows the optical micrographs and galvanic corrosion current density curves of coated (TU and TB) and uncoated Ti-6Al-4V alloy in the 3.5% NaCl solution. There were no changes of surface morphologies before and after the corrosion tests. Therefore, the Ti-6Al-4V alloy showed an excellent anti-corrosion property, which was also supported by the negligible ZRA current density value. The results indicated that the carbon fiber would not cause corrosion effects on Ti-6Al-4V. After the PEO treatment, the corrosion current of coated Ti-6Al-4V alloys were also extremely low; there were almost no difference between the coated and uncoated Ti samples. Thus, both coated and uncoated Ti alloys exhibited superior galvanic corrosion

resistance than steel and alumina when coupled with carbon fibers in salt corrosion media.

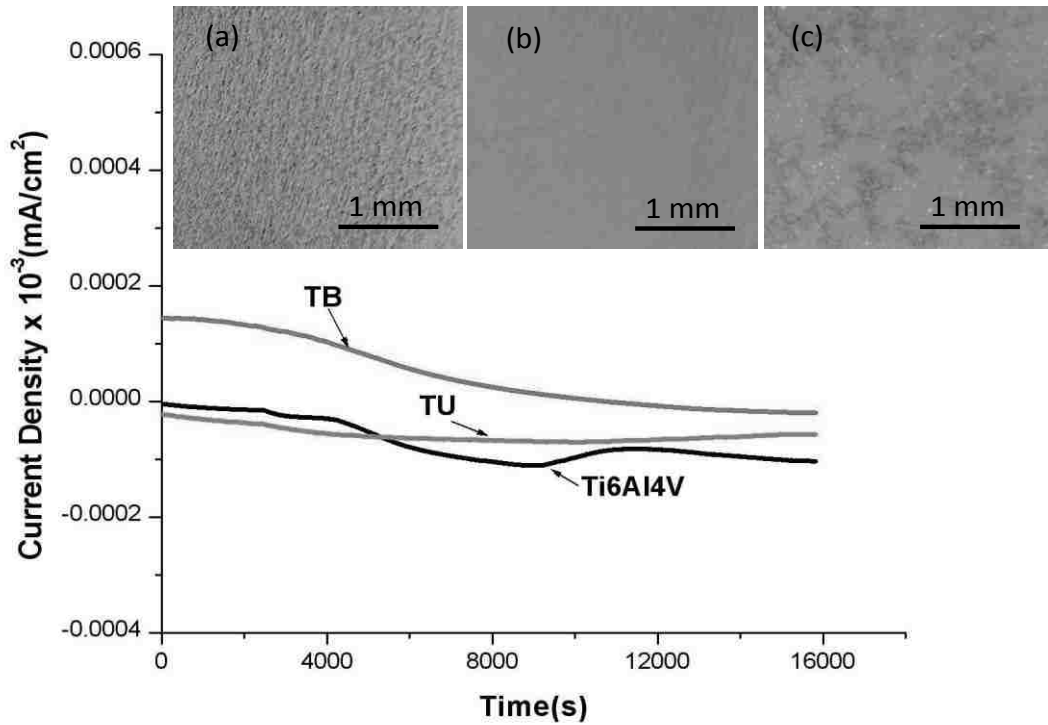


Fig. 5.5 The optical micrographs and galvanic corrosion current density of the test samples in the 3.5% NaCl solution for Ti6Al4V alloys: (a) un coated. (b) treated by a bipolar current mode (TB) and (c) treated by a unipolar mode.

It should be noted that making a uniform and adhesive PEO oxide coating on the steel for corrosion protection is still underway. More work is needed in the future to solve the non-uniformity issue of the coating. On one hand, the uncoated steel would have a corrosion problem when it is coupled with carbon fibers. On the other hand, it was not found that the uncoated Ti alloy had any corrosion concern under the testing environment, thus a PEO coating may not be

necessary for the Ti case. However, a PEO coating is much needed for the A356 aluminum alloy.

4. Conclusions

Different current modes during the PEO process were used to produce ceramic oxide coatings on an aluminum A356 sub strate. For the studied treatment conditions, the bipolar current mode would make the coating thicker than the unipolar mode. The potentiodynamic polarization corrosion test results showed that the ceramic PEO coatings significantly affected the corrosion polarization characteristics of the A356 alloy. The coatings prepared using duplex unipolar and bipolar treatments had a dense surface and as a result, showed the lowest corrosion current and highest corrosion resistance in the potentiodynamic polarization corrosion tests. The ranking for corrosion resistance in a 3.5% NaCl solution was steel<A356<Sample C<Sample D<Sample A<Sample B.

The ZRA test results suggested that when coupled with carbon fiber in the 3.5% NaCl solution, the steel and A356 aluminum alloys were severely corroded while the titanium alloy was almost intact. The ZRA tests also showed that all the coated samples had a much lower corrosion current density than the uncoated A356 alloy. Among the PEO ceramic coatings which could provide an efficient protection to the A356 alloy from corrosion of the 3.5% NaCl solution,

Sample B, prepared using combined unipolar and bipolar current modes, had the best performance in galvanic corrosion tests. For the Ti-6Al-4V cases, both coated and uncoated samples exhibited excellent galvanic corrosion resistances in the test environment.

Acknowledgment

The research was supported by the National Sciences and Engineering Research Council

(NSERC), and the Collaborative Research and Development (CRD) Program, Canada.

References

- [1] A Macke, B.F. Schultz, P. Rohatgi, *Adv. Mater. Process.* 170 (2012)19.
- [2] R.G. Boeman, N.L Johnson, SAE International paper. SAE: 2002-01-1905, 2002.
- [3] J.M. Corum, ORNL[fM-2000/322, Oak Ridge National Laboratory, <http://www.ornl.gov/-webworks/cpprJY2001/rpt/110550.pdf>, April 2001.
- [4] T.A Markley, M. Forsyth, A.E. Hughes, *Electrochim. Acta* 52 (2007) 4024.
- [5] A Afaghi-Khatibi, L. Ye, Y.W. Mai, *Compos. Sci. Technol.* 56 (1996) 1079.
- [6] H. Schmidt, A. Langenfeld, R. Na, *Mater. Des.* 18 (1997) 309.
- [7] M. Mandel, L. Kruger, *Mat.-wiss. u. Werkstofftech.* 43 (2012) 302.
- [8] Y. Fovet, L Pourreyron, J.-Y. Gel, *Dent. Mater.* 16 (2000) 364.
- [9] M. Tav akkolizadeh, H. Saadatmanesh, *Compos. Constr.* 5 (2001) 200.
- [10] E. Matykina, A. Berkani, P. Skeldon, G.E. Thompson, *Electrochim. Acta* 53 (2007) 1987.
- [11] AL. Yerokhin, X. Nie, A. Leyland, A. Matthews, S. Dowey, *Surf. Coat. Technol.*122 (1999) 73.
- [12] V.S. Rudnev, T.P. Yarovaya, D.L Boguta, LM. Tyrina, P.M. Nedorozov, P.S. Gordienko, J. *Electroanal. Cherm.* 497 (2001) 150.
- [13] S.V. Gnedenkov, OA. Khrisanfova, AG. Zavidnaya, S.L. Sin ebrukhov, A.N. Kovryanov, T.M. Scorobogatova, P.S. Gordienko, *Surf. Coat. Technol.* 123 (2000) 24.
- [14] Y.T. Sui, C.B. Johansson, S. Petronis, A. Krozer, Y. Jeong, A. Wennerberg, T.

Albrektsson, *Biomaterials* 23 (2002) 491.

[15] J.P. Schreckenback, G. Marx, F. Schlottig, M. Textor, N.D. Spencer, *Mater. Sci. Mater. Med.* 10 (1999) 453.

[16] R.O. Hussein, X. Nie, D. Northwood, A.L. Yerokhin, A. Matthews, *J. Phys. D Appl. Phys.* 43 (2010) 105203.

[17] R.O. Hussein, X. Nie, D.O. Northwood, *Surf. Coat. Technol.* 205 (2010) 1659.

[18] M.T. Mantas, R. Sanchez-Tovar, J. Garcia-Anton, V. Perez-Herranz, *Int. Electrochem. Sci.* 5 (2010) 1934.

[19] R.O. Hussein, D.O. Northwood, X. Nie, *J. Vacuum Sci. Technol. A.* 28 (4) (2010) 766.

[20] Z.J. Peng, Y. Chen, X. Nie, *Adv. Mater. Res.* 282-283 (2011) 774.

[21] P. Zhang, X. Nie, D.O. Northwood, *Surf. Coat. Technol.* 203 (2009) 3271.

CHAPTER 6

MOS₂/AL₂O₃ COMPOSITE COATINGS ON A356 ALLOY FOR FRICTION REDUCTION

1. INTRODUCTION

In order to reduce the fuel consumption and pollution, automotive companies are developing aluminum-intensive components. However, due to the low wear resistance of the aluminum (Al) alloys, Al cylinder bores are vulnerable to the sliding wear attack. Plasma electrolytic oxidation (PEO) is a promising surface modification technique for the improvement of the tribological properties of metals, such as Al, Mg, Ti and their alloys [1, 2, 3].

The PEO process is based on the interaction between the oxide film growing on the anodic metal and spark arc micro-discharges. PEO resembles anodizing, but it is significantly different because it makes much harder, thicker layers while using environmentally less harmful electrolytes [4]. PEO coatings have been studied for various applications, including those for which wear resistance, corrosion resistance and thermal protection are being sought. While PEO treatment imparted excellent features such as wear and corrosion resistance on aluminum and magnesium [5], there is still a huge challenge in how to reduce coefficient of friction for the tribological applications.

The inorganic solid lubricant molybdenum disulfide (MoS₂) is a kind of solid lubricant, which has extensively been applied to reduce friction for a long time. Its crystalline microstructures, tribological properties and anti-friction mechanisms have been studied deeply. There are lots of techniques for preparing a MoS₂ film, such as magnetron sputtering,[6, 7] ion beam assisted

deposition, anode oxidation combined with heat treatment, chemical reaction and high temperature annealing, as well as sol-gel method. The above techniques are useful, but obviously have the disadvantages such as inaccurate atomic ratio between sulfur and molybdenum and low deposition efficiency, or oxidation after high temperature annealing, or poor bonding strength with substrate.[8] While there are a number of published papers on PEO coatings on aluminum, reporting e.g. process characterization, physical and mechanical properties, tribological properties and thermo-optical properties, however, there has not been any concerted attempt PEO with MoS₂ coatings in relation to friction reduction and wear resistance.

In the present research, Plasma Electrolytic Oxidation (PEO) coating plus MoS₂ particles has been applied to the A356 alumina alloy through the electrophoretic deposition of MoS₂ particles. The alkaline electrolyte solution containing suspension of MoS₂ particles was used to prepare a composite film of MoS₂ and Al₂O₃. The resulting microstructural and tribological properties were examined via optical microscopy, scanning electron microscopy (SEM) and tribotests.

2. Experimental procedure

The material used in this study was cast A356 plates of 5 mm thickness, diameter was 2.6cm, with a nominal composition of 7.22 Si, 0.45 Mg, 0.15 Fe balance Al (in wt percent). MoS₂ powder (99% pure and 3µm average particle size) was used in this study. In this work, an electrolyte was prepared from a solution of sodiumsilicate (2-10 g/l) in distilled water with addition of KOH (1-2g/l) to adjust PH value and conductivity. A unipolar or bipolar pulsed DC voltage pulsed at a frequency of 50 Hz was selected in the range of 400 V in the positive half cycle and 100V in the negative half cycle; and a predefined current density (400 mA/cm²) at the coating surface was maintained during the process.

There were five samples adopted for this experiment. There was sample 1 to sample 5. Sample 1 was coated without MoS₂ for 10 minutes after reaching the peak voltage (unipolar 430V). Time to reach this Peak Voltage was 9.05 minutes. Sample 2 was coated with MoS₂ at first 5 minutes by 0.4A/cm². After that, the circuit current density was decreased by half (0.2A/cm²) and continue for another 5 minutes. Sample 3 was coated with MoS₂ at first 5 minutes and switch + and – pole (bipolar mode) and also the current was decreased by half for another 5 minutes. Sample 4 was coated with MoS₂ at first 5 minutes and then, switch + and – pole (bipolar) but keep the same current (0.4A/cm²) to another five minutes. For sample 5, the sample was coated in the electrolyte containing MoS₂ powders, after the voltage reached the peak voltage (unipolar 430V), the coating process was continued to another 10 minutes.

A pin-on-disc tribometer was occupied to evaluate tribological properties of those samples at dry and lubricated conditions with 1 N and 2 N normal loads, and 50 m sliding distance with steel balls (AISI 52100) as counter pins. For lubricant testing conditions, small amount of 5W10-30 engine oil was applied on the testing sample surfaces to simulate a boundary lubricant condition. Scanning electron microscopy (SEM), FEI Quanta 200 FEG microscope, operating at 20 keV, with an energy dispersive x-ray analysis system (EDX) was used to analyze the coated samples. The profilometer was used to provide areas of cross-sections of wear tracks from which the wear rate k can be defined as the volume loss per unit sliding distance and normal load, which be calculated and determined by the expression:[9]

$$k = \frac{\text{Volume loss}}{\text{Normal load} \times \text{Sliding distance}} = \frac{A \times L}{N \times I} \quad \text{Eq. 6.1}$$

A and L are the cross-sectional area and length of wear track, respectively. N is the load, I the sliding distance.

3. Result and Discussion

The coefficients of friction of those samples were acquired and calculated. The result showed on Fig. 1. after smoothed. The substrate and Samples 1-4 all exhibited a high coefficient of friction during the tests at the first 10-15 m sliding distance (around 1000 revolutions). However, unlikely the substrate S1 and Sample 1 (without MoS₂), Samples 2, 3, 4 and 4 had a lower ramped up friction, which may be caused by a small amount of MoS₂ in their coatings.

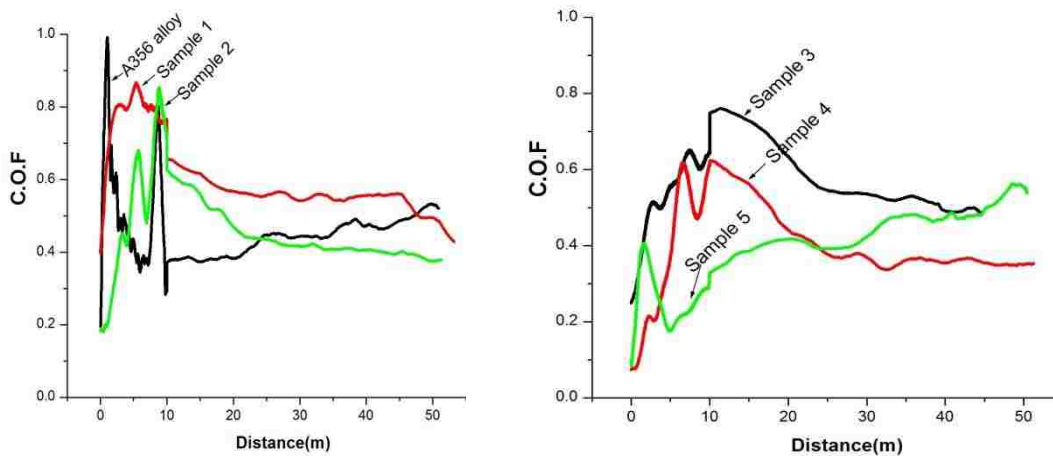


Fig. 6.1. C.O.F. curves of (a) A356, S1 and S2 and (b) S3, S4 and S5 at 2N & 50m dry test conditions.

Sample 5 exhibited the lowest C.O.F (0.18-0.28) among all samples during the initial 10m dry pin-on-disc test, indicating that more MoS₂ likely existed in the PEO coating and acted as a solid lubricant. It can be found in Fig 1 that at the end of the wear test, the C.O.Fs had a similar value under the 2N load. The reason for this is that the coating layers had been broken due to the high load. To further investigate the wear performance improved by adding MoS₂, Sample 1 and Sample 5 were chosen to do another run of pin-on-disc tests under 1N load for 50m, Fig. 6.2. After the tests, both Al₂O₃ (Sample 1) coating and composite MoS₂/Al₂O₃ (Sample 5) coating samples were investigated by using SEM and EDX, Fig. 6.3. From the SEM and EDX results, it

can be seen that although the wear track widths for Sample 1 and Sample 5 were almost the same, the compositions for wear tracks were different. Fe oxides were found in both sample's wear tracks. A higher brightness of transferred materials on Sample 1 should indicate the Fe was oxidized to a larger degree than the transferred Fe on Sample 5. The EDX analysis result also showed that the percentage of Mo/S element was around 0.3%-1.75%. The MoS_2 and the less oxidized Fe (may being FeO) can reduce coefficient of friction for Sample 5 [10-11]. As a result, Sample 5 had a lower C.O.F than Sample 1, Fig.6. 2.

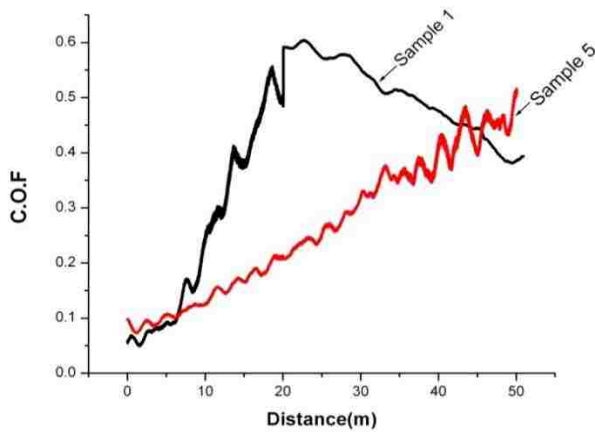


Fig. 6.2. C.O.F. curves of (a) S1 and (b) S5 at 1N and 50m dry test conditions.

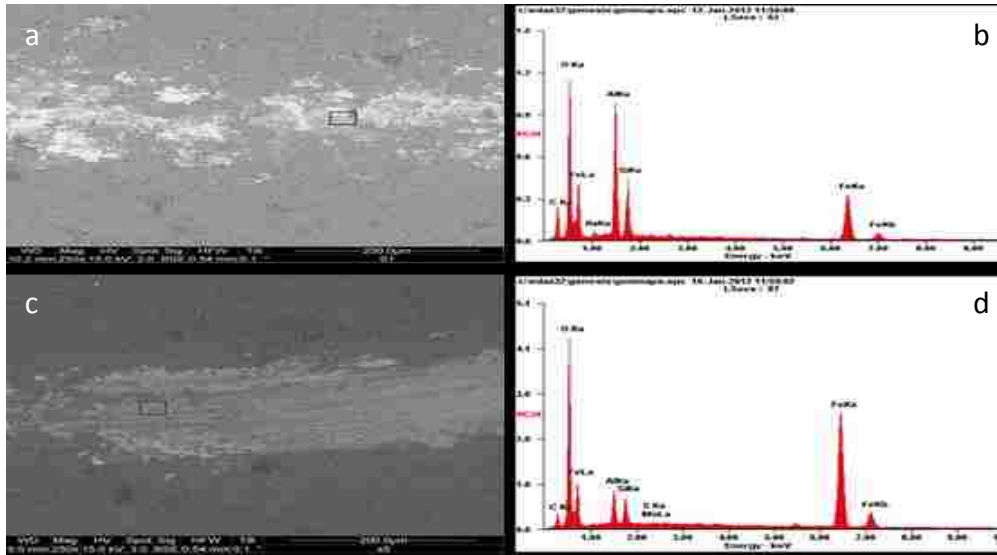


Fig. 6.3 SEM micrograph and EDX spectra of coatings on (a, b) Sample 1 (without MoS₂) and (c, d) Sample 5 (with MoS₂)

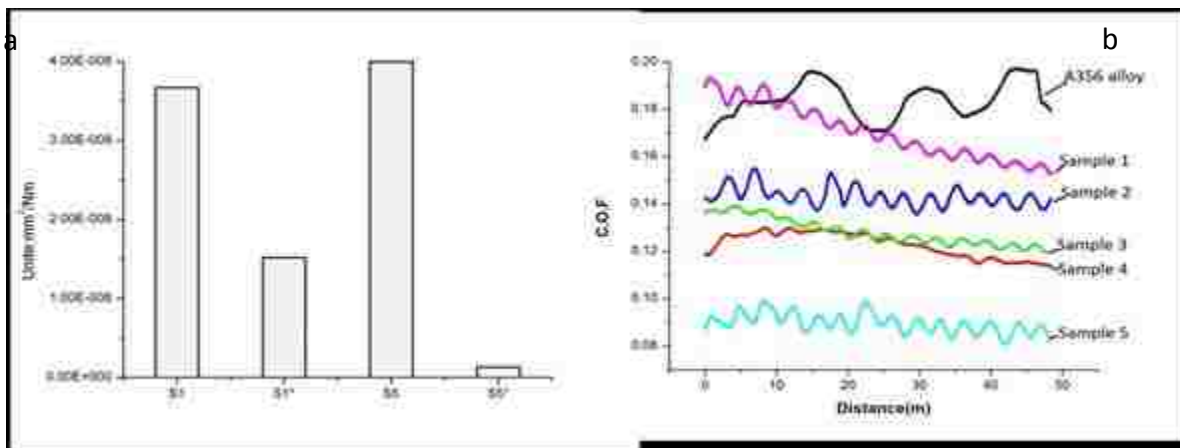


Fig. 6.4 (a) Wear rates of samples S1 and S2 under the pin-on-disc dry test conditions for both 2N and 1N (labeled with*) loads, and (b) Tribological behaviours of A356 and coated samples under lubricant test conditions at a 2N load for 50m (4000 revolutions).

Fig. 6.4(a) shows the wear rates of samples S1 and S5 under the pin-on-disc dry testing conditions at 2N (labeled as S1 and S5) and 1N (labeled as S1* and S5*) loads. The 2N load test conditions caused both coatings on S1 and S5 failed while the coatings were still intact under 1N

load conditions as shown in Fig. 6.3. When the coating surfaces were broken, the Al_2O_3 particles from the broken coatings would be attached on the surfaces of the steel ball and substrate and formed third body abrasive wear which caused the high wear rate. However, when the load changed to 1N, the wear rate of Sample 5 was obviously lower than that of Sample 1. It suggested that MoS_2 played a significant role in this experiment.

SEM observations also showed that both coatings consisted of a porous surface layer, which may be useful as lubricate oil retaining dimples during lubricate tests. Fig. 6.4(b) shows the C.O.F.s under the lubricant testing conditions where the MoS_2 -coated samples (Samples 2-5) had a significantly lower C.O.F. (by 0.11) than the aluminum substrate. Sample 5 showed the lowest C.O.F. Thus, the coatings with MoS_2 again performed better than the uncoated and Al_2O_3 only coated substrates under lubricant test conditions. In terms of both friction coefficient and wear resistance, the benefit from the MoS_2 seems become more obvious in the lubricant than in dry test conditions.

4. Conclusions

Al_2O_3 and $\text{MoS}_2/\text{Al}_2\text{O}_3$ coatings were prepared using a Plasma Electrolytic Oxidation (PEO) process at both unipolar and bipolar pulsed-DC modes. All samples coated with Al_2O_3 plus MoS_2 showed a lower C.O.F. than the uncoated substrate. While the Al_2O_3 coating without MoS_2 exhibited a high coefficient of friction, C.O.F = 0.5-0.6, the MoS_2 incorporating with the Al_2O_3 coating would reduce the C.O.F to 0.18-0.28 before the coatings failed. The $\text{MoS}_2/\text{Al}_2\text{O}_3$ coating appeared to have a longer wear life than Al_2O_3 -coated and uncoated A356 alloys. Under the lubricant testing condition, the $\text{MoS}_2/\text{Al}_2\text{O}_3$ composite coatings also had a significantly lower C.O.F. than the uncoated and Al_2O_3 -coated aluminum substrates. Therefore, the solid lubricant

MoS₂ demonstrated its role in the composite coatings with respect to a lower friction coefficient and wear rate than both original and Al₂O₃-coated alumina alloys.

References

- [1] X. Nie, E.I. Meletis, J.C. Jiang, A. Leyland, A.L. Yerokhin, A. Matthews: Surface and Coatings Technology 149 (2002) 245–251
- [2] A. Yerokhin, X. Nie, A. Leyland, A. Matthews: Surface and Coatings Technology, 130 (2000) 195-206
- [3] X. Nie, A. Wilson, A. Leyland, A. Matthews U., Surface and Coatings Technology, 121 (2000) 506-513
- [4] X. Nie, L. Wang, E. Konca, A.T. Alpas: Surface and Coatings Technology, 188–189 (2004) 207-213
- [5] H.S. Ryu, S.J. Mun, T.S. Lim, H.C. Kim, K.S. Shin, S.H. Hong: J. Electrochem. Soc., 158 (2011) C266-C273
- [6] H. Wang, B. Xu, J.J. Liu, D.M Zhuang: Science and Technology of Advanced Materials 6 (2005) 535–539
- [7] X.D. Zhu, W. Lauwerens, P. Cosemans, M.V. Stappen, J.P. Celis, L.M. Stals, J.W. He: Surface and Coatings Technology, 163–164 (2003) 422.
- [8] D.M. Zhuang, J.J. Liu, B.L. Zhu, W.Z. Li: Wear, 210 (1997) 45
- [9] X. Nie, L. Wang, Z.C. Yao, L. Zhang, F. Cheng: Surface and Coatings Technology, 200 (2005) 1745 – 1750
- [10] M.M Chen, J. Lin, T.W. Wu, G. Castillo: Journal of Applied Physics, 63 (1988) 3275 - 3277
- [11] R. L. Deuis, C. Subramanian, J. M. Yellup: Composites Science and Technology, 57 (1997) 415-435

Chapter 7

EFFECT OF PLASMA ELECTROLYTIC OXIDATION COATINGS ON FRICTION AND WEAR BEHAVIOR OF ALUMINUM ENGINE CYLINDER BORES

1. Introduction

Aluminum casting alloys which contain silicon show great potential for engine cylinder applications as they impart excellent castability, low density, and good mechanical properties. Aluminum alloys have been used for tribological engine applications in the last few years, examples are A390, AlusilTM, SilitecTM, LokasilTM, etc. [1–3]; those alloys are all hypereutectic alloy which contain 17–25 wt. % Si. Currently, only luxury vehicles are produced with linerless engine blocks made of hypereutectic aluminum-silicon (Al-Si) alloys. The cheaper eutectic and near-eutectic aluminum–silicon alloys do not usually appear to have a strong surface to withstand wear problems caused by piston rings; a cast iron liner or thermal spraying coating is used for improved tribological properties of Al-Si casting alloys with a low Si content.

The wear mechanisms, wear regimes and transitions of Al-Si alloys have been investigated in the past [4-9]. Those researches have shown that aluminum does not exhibit sufficient wear resistance to maintain cylinder wear among the ultra-mild wear regime. For that reason, by means of alloying and the addition of hard particles wear resistance can be promoted. The actual role that the microstructure, and specifically the hard phases and particles, act in providing wear resistance in aluminum casting alloys is a useful solution for wear. As a result, the effect of silicon content and morphology on wear resistance has been the main focus of many studies [10–

12]; these studies give information that smaller eutectic silicon particles provide the stiffest resistance to particles sinking-in. Engine bores show to undergo microstructural transformations which are kind of element of their wear resistance. However, engine tests performed on hypereutectic parent metal engine bores [13, 14] report that the general knowledge that the hard particles simply carry the entire load is not the correct solution. Instead, recent researches indicate that the combination of brittle, hard phases, plus a ductile matrix, and the breakdown products of the oil with the oil additive package cause to a very complex surface structure when subjected to cyclic sliding loads at or close the shear strength of the aluminum matrix. This surface microstructure, which is not similar with the initial surface preparation, should have suitable wear resistance for long-term engine bore durability applications. [15]

Plasma Electrolytic Oxidation (PEO) method is considered as an environmentally and cost-effective electrochemical process, which can make a wear resistant oxide film on a variety of metals [16-19]. Different from the general anodizing process, PEO adopts a voltage above the dielectric breakdown potential of the oxide layer, which causes the gas evolution and local formation of plasma [20]. The PEO coatings are much harder than the anodizing coatings. Moreover, the PEO process uses dilute alkaline solutions instead of acidic electrolytes, which is less harm to the environment. Therefore, it is reasonable to apply the PEO process to the engine cylinder bores of the all Al engine block to provide sufficient wear protection without causing any environment hazard.

Previous researchers mainly focused their studies on the wear resistance of PEO coatings on Al alloys that are not cut from real casted engine blocks [21–25]. Research on the wear performance of the PEO coatings on Al under the lubrication condition was very limited. Investigation in the wear properties of PEO coatings on Al alloys under the starved and boundary lubrication

conditions were reported in references [26, 27]. It was found that the micro porosities on the coating surfaces can be acted as oil reservoirs and were beneficial to the oil-lubricated wear performance. However, comparison between the wear performance of PEO coatings and materials used as the commercial engine cylinder bores has not been reported yet. Generally, a thick, dense and smooth PEO coating is desirable for tribological applications. However, as the coating thickness is increased, the PEO coating forms a porous and rough outlayer on the top of a dense inner layer. The worn off hard debris from the coarse outlayer would cause abrasive wear to both the cylinder bores and the piston rings. It is necessary to smoothen the coating surface when the coating is thick. In order to acquire a honing-free coating through short treatment time for cost saving, relatively thin PEO coatings were prepared in this work. The thin coatings with tailored surface morphology and coating thickness were studied in tribological properties, compared with commercially available engine cylinder bore materials.

2. Experiment method

A PEO coating unit as described in Ref. [28] was used to produce the oxide coatings on the Al cylinder bore. The electrolyte was mainly sodium aluminate (6-8g/l NaAlO_2) with a small amount of potassium hydroxide (KOH) added to balance the pH at 11. A small amount of MoS_2 powders (2-3 g/l) also was added to the solution. During the PEO process, the Al cylinder bore as the anode and a stainless steel plate as the cathode were connected to a unipolar pulsed DC power supply. 80% of the duty cycle and 2 kHz frequency were used for the high coating growth rate [29]. There were two coatings prepared on the Al cylinder bores which were 5 minutes and 10 minutes, respectively. Average surface roughness R_a of the coated Al cylinder bores was measured by a Mitutoyo SJ-201P stylus surface profiler. A scanning electron microscope (SEM JEOL-5800LV) with energy dispersive X-ray analysis (EDX) was utilized to

observe surface morphologies of the specimen cut from the coated cylinder bore's and commercial cylinder bores including Alusil, PTWA, and casting iron.

Tribological properties of all the cut specimen were investigated using a reciprocating sliding tribometer against AISI 52100 chrome steel balls which were 4 mm in diameter. Vickers hardness for the balls was about 700 HV. Made of hypereutectic Al–Si alloys, Alusil specimen was prepared from a commercially available Alusil® engine cylinder liner which was machined with a special honing process to allow the Si particles in the Alusil alloy protruded from the matrix and were designed to isolate the contact between the soft matrix and the wear materials. However, for the real case, the engine cylinder bore could still undergo considerable wear loss under the following circumstances: cold start, the use of the ethanol–gasoline mixture fuel (E85) and the directly injected fuel, where direct friction surface contacts would happen due to the lack of the oil lubricant. Therefore, in order to evaluate the anti-wear performance of the PEO coatings on cylinder bore in those worse cases, the wear tests were conducted under the starved lubrication conditions of 5W20 Motomaster engine oil where friction countersurfaces contacted at their micro-asperities due to lack of formation of lubricant film. A normal load 15 N was selected so that the reference Alusil, PTWA and casting iron samples experienced between the mild wear and severe wear [30]. The sliding distance was 1000 m for those samples. For a dry without lubricant condition, PTWA coated sample and PEO coatings prepared in electrolytes containing a solid lubricant powders or without the powders were tribotested at 1N load and 100m sliding distance. The wear tracks on the PEO coatings and those reference samples were studied using SEM. A Buehler Omnimet optical microscope was utilized to observe the wear tracks on not only the coated sample but also reference samples and the worn areas of all the steel balls. All coating samples were slightly polished (similar to a

brushing process) to Ra value below 0.5.

3. Results and discussion

Fig.7.1 shows the optical micrographs of the wear tracks on the PEO coating samples and scratched scars on the steel balls as well as friction curves at the boundary oil lubricant condition. Fig. 1(a) is for ta PEO coating S1 prepared with a powder-contained electrolyte for a relatively long treatment time (10 minutes). Fig. 1(b) is for a PEO coating S2 treated for a short time (5 minutes). Fig. 1(c) depicts a PEO coating S3 prepared in the electrolyte without the MoS₂ powders. In each picture, mark (i) is for wear track of the coating, (ii) for scratch scar on the steel ball and (iii) the coefficient of coefficient (C.O.F). From those pictures, it is shown that the coating S3 which was prepared in the no-powder contained electrolyte shows a higher C.O.F than the other two coatings. The C.O.F of the coating S3 went up to maximum 0.24 which is much higher than the coatings prepared in the electrolyte with powders. Usually, the surface of PEO coating is uniformly distributed with many micro-pores and dimples of the sizes ranging from a few to several micrometers. Previous research [31, 32] investigated that micro-pores were formed by the molten oxide and gas bubbles thrown out of micro-arc discharge channels. For oil-lubricated sliding condition, micro-pores, micro-cracks or dimples which were normally deliberately produced on the wear surface, can alter the hydrodynamic efficiency and hence lubrication regime or performance of sliding surfaces [33, 34]. These pores and dimples on PEO coating can act as reservoirs for oil lubricants, which may result in a positive effect to the tribological performance of PEO coatings under boundary lubricated conditions. However, in this case, the load is 15N which is much higher than previous tests. The wear track picture in Fig. 1(c) shows the coating S3 was locally broken at one end of its sliding tracks where the sliding

speed was slower and thus oil lubricant condition become even worse than the center area of the wear tracks. The oil film discontinuity could not keep the oil staying in the counter face between wear surface and steel ball.. The wear track width is around 500 μm and the worn area for steel ball is $468 \times 571 \mu\text{m}$.

On the contrast, when a PEO coating was treated has in powders-contained electrolyte, the pores which were generated during the plasma discharges could be filled with powders. The powers were solid lubricant which can to some extent provide a lubricating effect. Thus, the coatings S1 and S2 exhibited a lower C.O.F than the coating S3. Compared the coating S1 (the long time treated sample) with the coating S2 (the short time treated sample), it can be found that the wear track of S1 is slightly larger than that of S2. me one and worn surface for these two work piece However, the sizes of wear scars of the counterface balls are almost the same. For the C.O.F, the PEO sample S2 had a stable friction coefficient curve which is not larger than 0.13. The coating sample S2 had an increased C.O.F. curve from 0.14 to 0.16 and the localized coating was slightly ground off at the end of wear track. The reason for this phenomenon might be caused by treatment time. When the coating time was longer, although the coating thickness increased, , the long treatment time could cause the coating surface feature coarse. As a result, when the load was high, such as 15N, the coating would have more contact with steel ball, leading to a higher C.O.F. .

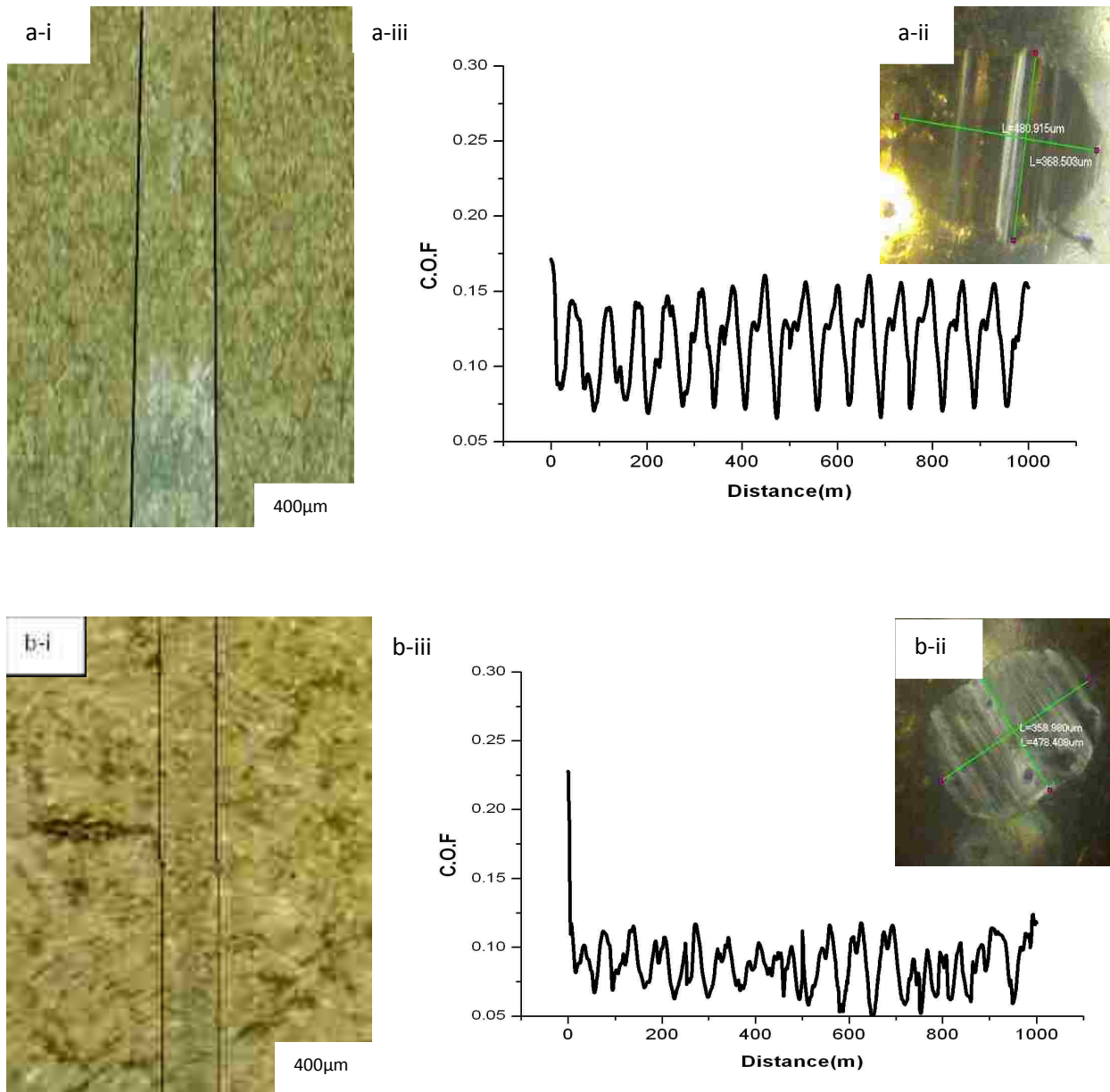


Fig 7.1. Optical micrographs of (i) the wear tracks on PEO coatings and (ii) wear scars on counterface steel balls, and (iii) C.O.F. for (a) Coating S1, (b) Coating S2, and (c) Coating S3 (continued)

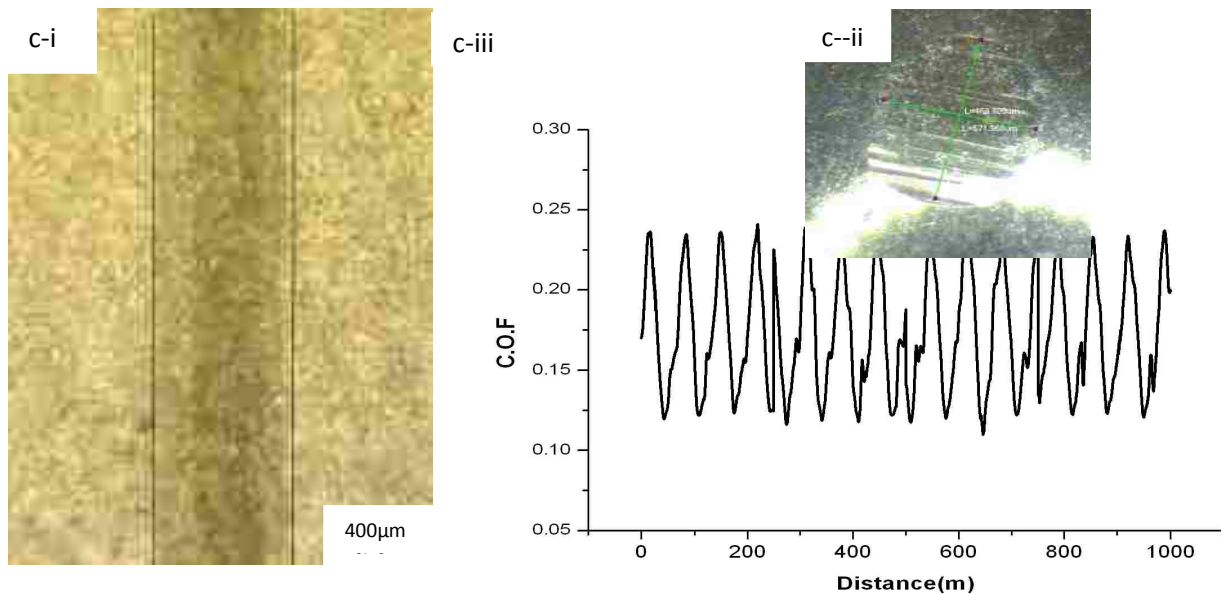


Fig 7.1. Optical micrographs of (i) the wear tracks on PEO coatings and (ii) wear scars on counterface steel balls, and (iii) C.O.F. for (a) Coating S1, (b) Coating S2, and (c) Coating S3..

Fig. 7.2 show the optical micrographs of the wear tracks on the reference samples and wear scars on the counterface steel balls. Fig.7.2(a) is for PTWA sample,. Fig.7.2(b) for Alusil® sample, and Fig.7.2(c) for cast iron sample. In each picture, mark (i) is for wear track, (ii) for scratching on steel balls and (iii) coefficient of friction (C.O.F).

Plasma transferred wire arc (PTWA) thermal spraying is a thermal spraying process that deposits a coating on the internal surface of a cylinder, or on the external surface of a part of any geometry. It is known for its use in coating the cylinder bores of an engine, enabling the use of aluminum engine blocks without the need for heavy cast iron liners. For Al-Si alloy engine blocks, PTWA provides a weight-saving alternative to cast iron liners, while delivering increased displacement in the same size engine package and a potential for better heat transfer.[35, 36] From Fig. 7.2(a), it can be found that there are honed grooves in the PTWA coating. Those microvalleys or grooves act as wear debris traps and oil reservoirs for the

lubricant. Those grooves can keep the oil on the coating surface during the wear test which causes the C.O.F as lower as the PEO coating S2 prepared in an electrolyte with solid lubricant powders for a short treatment time. However, the counterface wear was smaller than the case for the PEO coating which had a rough surface than the PTWA coating. The PEO coatings had a surface roughness $R_a = 0.5-0.6 \mu\text{m}$, and roughness of the PTWA coating was $R_a = 0.2 \mu\text{m}$.

The Alusil aluminium alloy is commonly used to make linerless aluminium alloy engine blocks. Alusil, when etched, will expose a very hard silicon precipitate. The descended aluminium matrix surface can hold oil, and silicon grains provide the load bearing surface.[37] Fig.7. 2(b) presents the tribotest results of Alusil sample. After a certain running time Si grains and the Al matrix were at the same height level. The steel ball was not only supported by the Si grains but was interacting with the Al matrix as well. The roughness of the original surface of the Al matrix might increase during the running of the test. As a result, the C.O.F. increased occasionally. The phenomenon could be observed for the PTWA case, except for the deferred time when the increased C.O.F. occurred at a 490-520 m sliding distance instead of 230-280 m for Alusil sample. The relatively soft Alusil and its smooth surface ($R_a = 0.2 \mu\text{m}$) were beneficial to the less counterface wear, compared to the PEO coatings, although the counterface wear appeared larger for Alusil than for PTWA and cast iron. The hard Si and possibly fractured Si grains may cause the slightly large wear scar on the steel ball.

Generally cast irons have good wear resistance. Cast irons are used in slurry pumps, brick dies, several mine drilling equipments, rock machining equipments and the similar areas [38, 39]. Cast irons have wide applications in diesel engines as engine block materials and in gasoline engines as liners for aluminium engine blocks. Fig.7. 2(c) shows the cast iron liner specimen tested at a 15N load, 1000m sliding distance and boundary oil lubricant condition. The cast iron had carbon

graphite in it, which may be the reason why cast iron exhibited a lower C.O.F. than PTWA. The surface areas weakened by graphite structures may be locally fractured, causing the relatively large scratching scar on the ball surface, compared to the PTWA coating.

In contrast with the PEO oxide coating, all the reference samples were relatively soft metallic materials with smooth surface finish, which resulted in less counterface wear. The previous research regarding surface roughness effect of a PEO coating on counterface wear indicates that the PEO coating with reduced roughness can have a similar or even smaller counterface wear [27] compared to the PTWA coating. On one hand, the strong PEO coating had an even C.O.F. curve without a spike, which may suggest the PEO coating have a better resistance to scuffing wear and the tribological property of the coating could be further improved with the increase of the running time due to the application-induced polishing effect. On the other hand, the metallic based coating or bore materials would be degraded during the application, and the frequency of

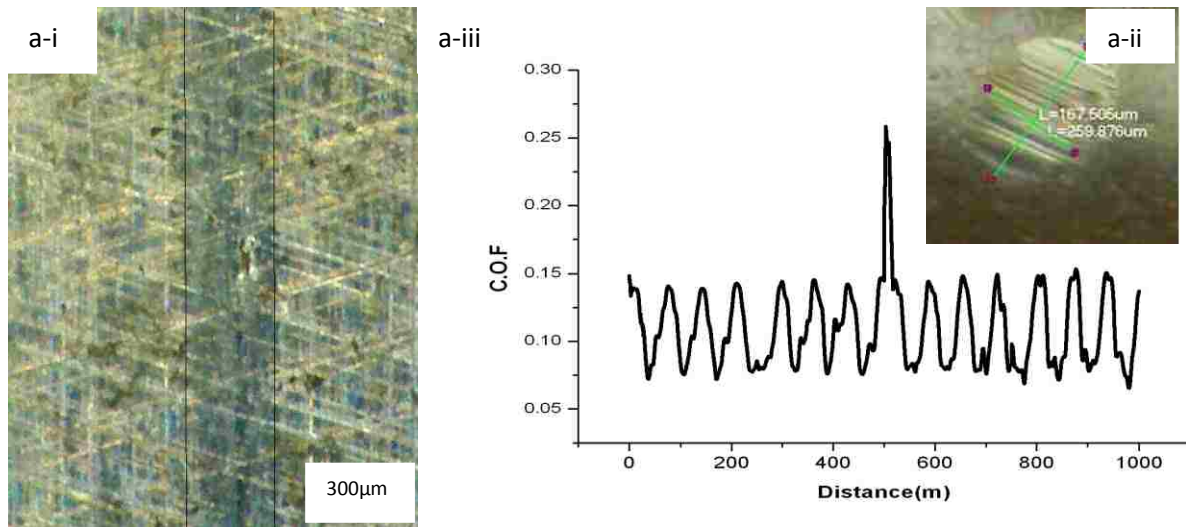


Fig. 7.2. Optical micrographs of (i) the wear tracks on reference samples and (ii) wear scars on counterface steel balls, and (iii) C.O.F. for (a) PTWA coating, (b) Alusil, and (c) cast iron (continued).

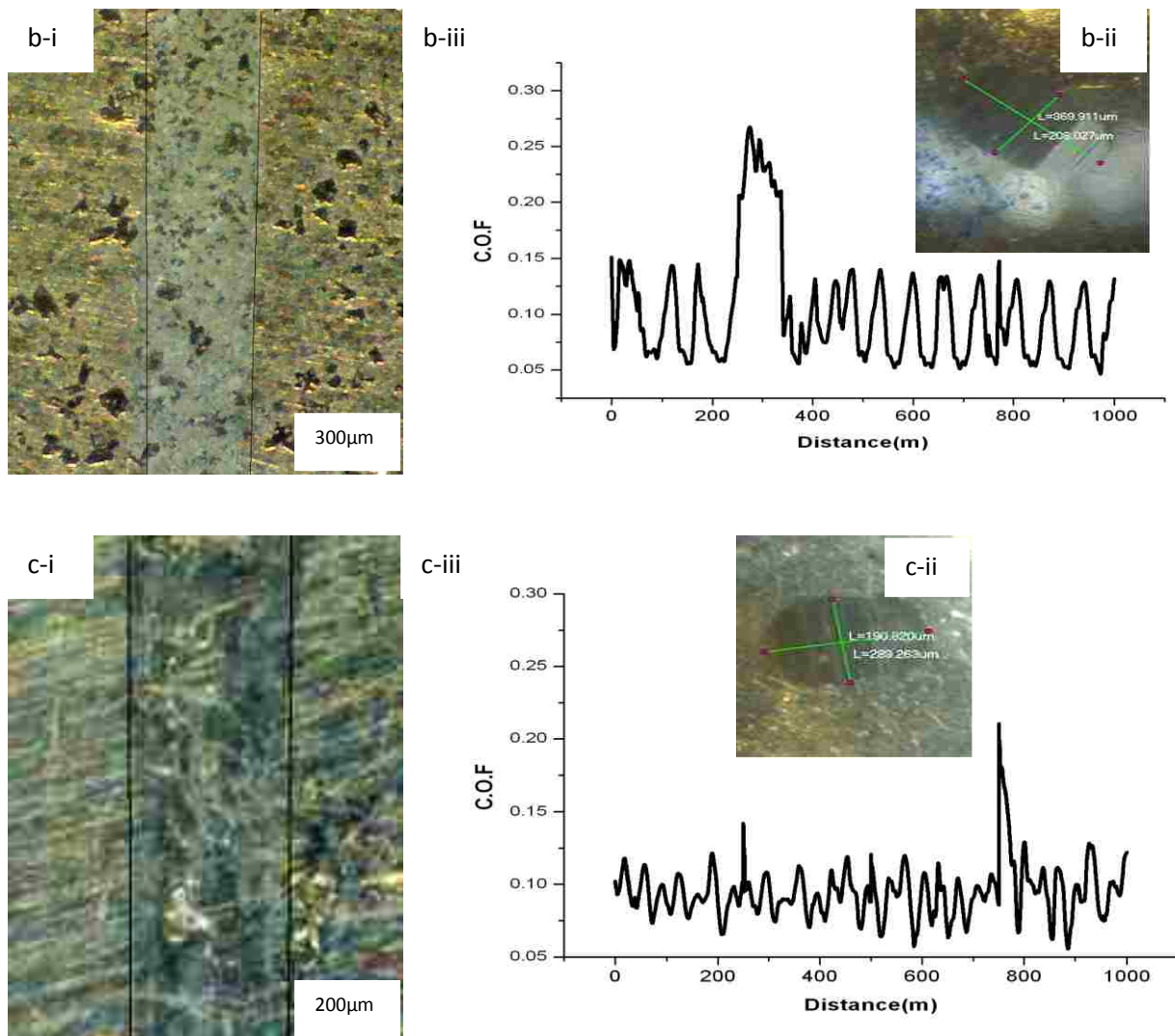


Fig. 7.2 Optical micrographs of (i) the wear tracks on reference samples and (ii) wear scars on counterface steel balls, and (iii) C.O.F. for (a) PTWA coating, (b) Alusil, and (c) cast iron.

appearances of spikes (i.e., high C.O.F.s) in the C.O.F. curves would be increased. SEM micrographs wear tracks of the PTWA sample are presented in Fig. 7.3(a) and 3(b). Surface fatigue turned out as delamination of individual fractures of splats. The coating cohesion was mainly provided by interlocking of splat particles and adhesion strength. Crack propagation

followed the splat boundaries where smooth surfaces hindered mechanical interlocking and finally perpendicular micro cracks could remove a splat particle from the surface. At a low rate this must not be detrimental because the open volume can store motor oil and favor lubrication. One has to notice that delamination of splats can already occur in the course of honing. A differentiation during which stage, manufacturing of the surface or engine operation, a splat particle is removed is unlikely when the steel ball slides over and modification of the surface is progressed. Another wear mechanism within this wear test was found to be an abrasion wear. Grooves of different width could be seen in sliding direction of the moving steel ball all over the surface. The honing texture was abraded completely. The SEM images (Fig.7.3(c)) can be used to explain the C.O.F curve for PTWA sample at a boundary lubricate, 15N load and 1000 m M sliding distance condition. At around 500m, the C.O.F value had a mutation up to 0.25 which was caused by deformation of splat particles. However, the damage was not very severe at the oil lubricated condition. As a result, the C.O.F. curve was drawn back to the origin value.

SEM images of wear tracks of the Alusil sample are presented in Fig. 7.3(d) and 7.3(e). It can be seen that the Al matrix was strongly modified during the wear test. A friction induced wear particle dispersion strengthening process is considered responsible for the enhancement of the wear resistance of the hypereutectic Al-Si alloy. The initial protrusion of Si primary particles is believed necessary to direct the energy input into the Si grains and to separate the steel ball from the initial contact to the soft Al surface. However, after the wear test, the elemental composition of the worn Al surface contains large amounts of oxygen, calcium and carbon, Fig. 7.3(f). Together with embedding of wear particles the aluminium matrix was plastically deformed. The C.O.F. curve in Fig.7.2(b) shows that the friction went high at around 300m sliding distance and then returned to normal at 400m.

SEM micrographs for wear tracks of the cast iron sample are presented in Fig.7.3(g) and 7.3(h). The cast iron specimen was tested against the steel ball under the same boundary lubricate conditions and for the same wear distance as the other cases. The wear tracks seem smoother and narrow. However, there were still cracks that appeared on the wear track surface. The cracks were believed initiated from graphite sites after the sample experienced with a relatively long sliding distance. As a result, the suddenly increased C.O.F. only appeared after the 800m sliding. The C.O.F. dropped back to its early level at 900m, indicating the sample did not have a severe scuffing problem yet.

The SEM observations and EDX analysis were also conducted for the wear tracks on the two PEO coatings after the sliding tests against chrome steel balls under a normal load 15 N for 1000 m. Fig. 7.4 shows the SEM micrographs of the wear track on the short time coated substrate (sample S2) and EDX spectra at two typical surface areas. Surface polishing was the coating wear mechanism, Fig.7 .4(a). The smoother areas with grey color were originally Al matrix, and the porous surface areas with bright color were related to Si-enriched regions (Fig.7 .4(b)). The EDX spectra still shows high contents of oxygen in all the areas within the wear tracks, Fig.7 4(c), which indicates the PEO coating was not broken. Element Mo could be found in the spectra a well, suggesting the solid lubricant powders MoS_2 might be physically or chemically collaborated into the coating particularly at the rough surface areas where the powders could stay in the pores. Unfortunately, only a few powders can be observed in or near pores. Therefore, a chemical reaction of Mo into the oxide coating might also occurs. The MoS_2 or Mo had seemingly played a role in the reduced C.O.F., compared to the PTWA coating. Although the test load is high (15N), the thin coating still can undergo the steel ball at a boundary lubrication.

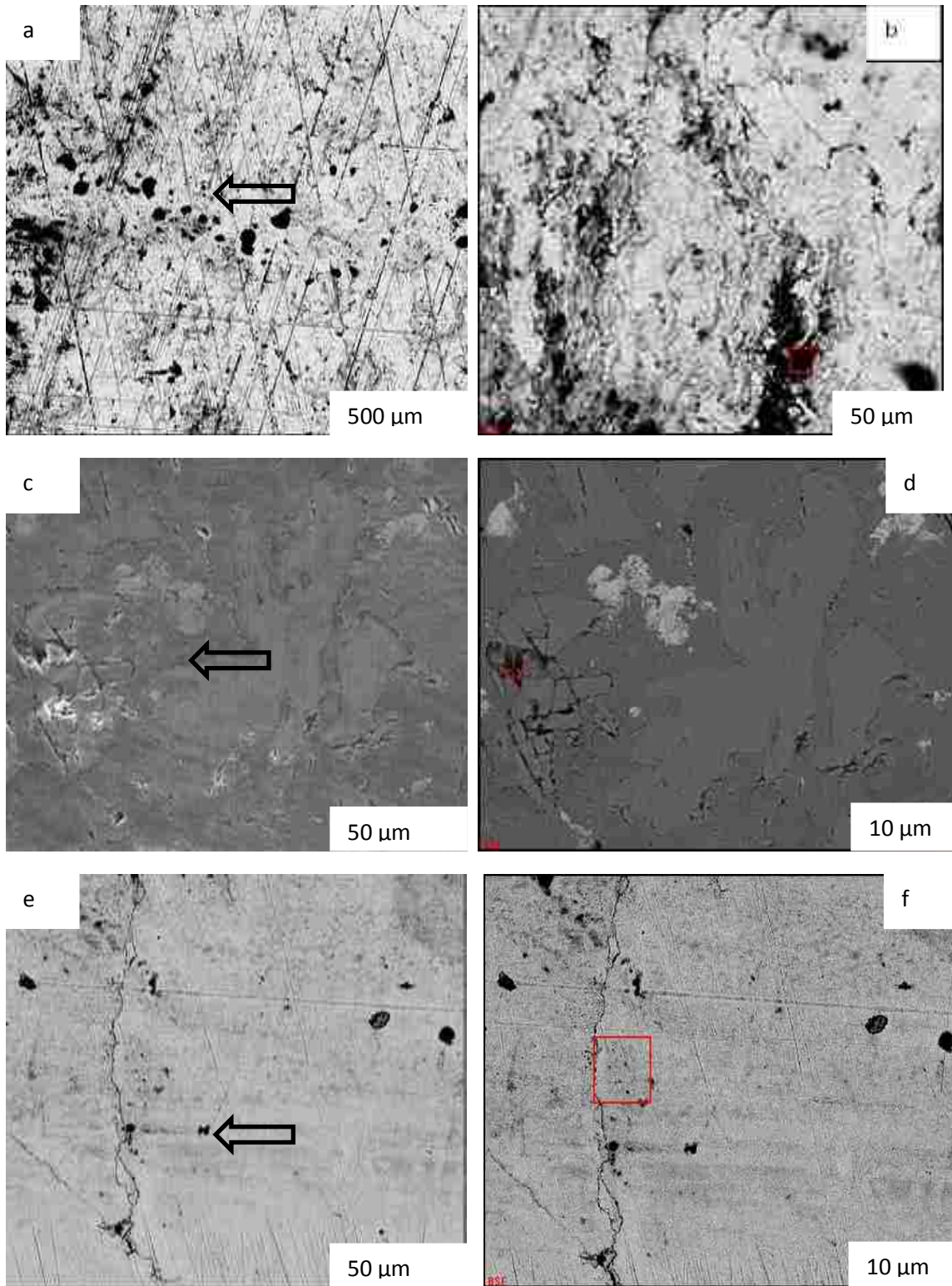


Fig. 7.3 SEM micrographs for (a, b) PTWA, (c-d) Alusil and (e-f) cast iron liner specimen after the tribotests.

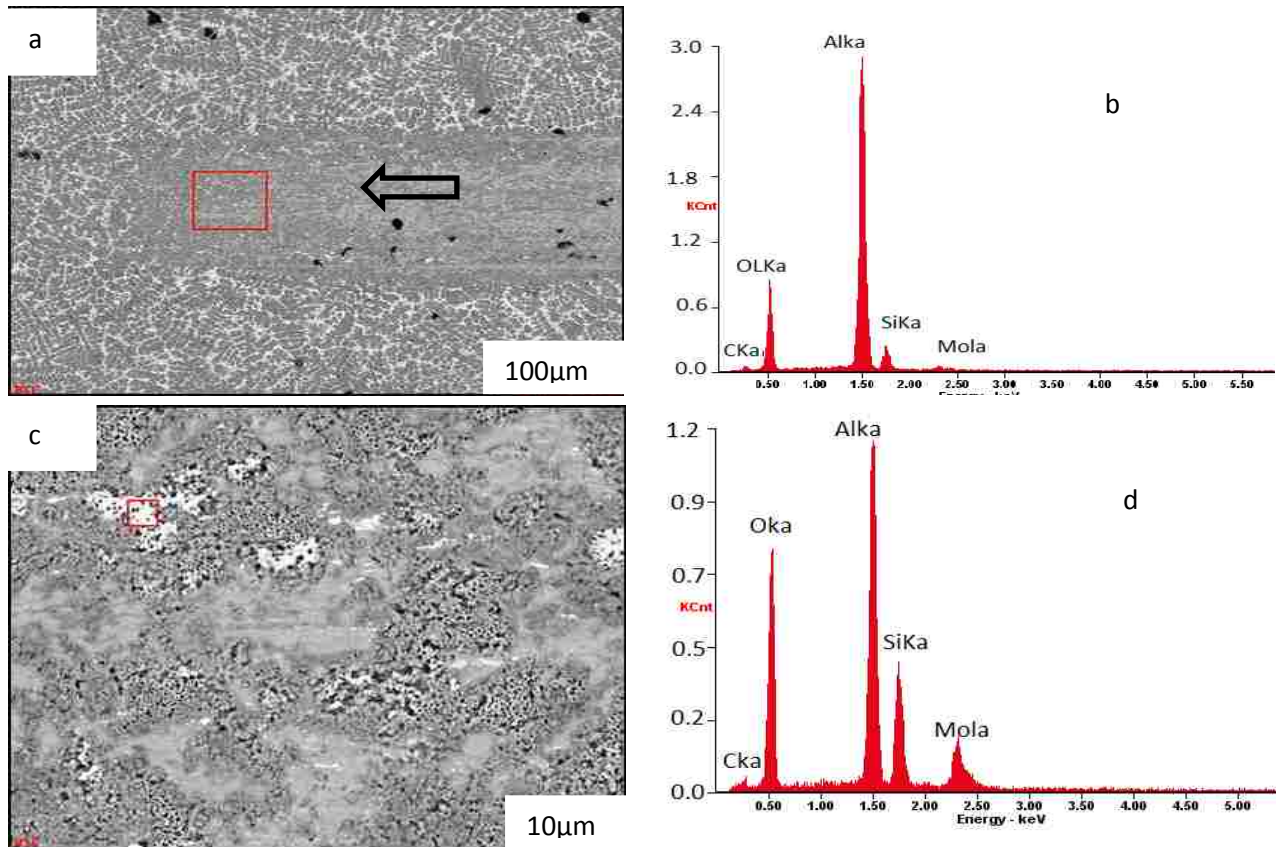


Fig.7.4 SEM micrographs and EDX spectra of the coating S2 after tested at a 15N, 1000m and oil lubricant condition.

Fig. 7.5 shows the SEM micrographs and EDX spectra of the wear track on the long time coated Al substrate S1. . A few tiny scratches and localized coating chipping off could be observed. The chipping off of the coating mostly occurred in the Si-enriched regions. The content of oxygen and molybdenum were higher in the coating S1 than in the coating S2 due to the longer treatment time. The EDX result may indicate more molybdenum powders existed in the pores which were produced by plasma charges. Although the PEO coatings were thin, the coatings can still withstand the high contact stresses (in a range of 800-1000 MPa maximum Hertz contact stress) of the tests at 15N load where the maximum Hertz contact stress was in a range of 800-1000 MPa.

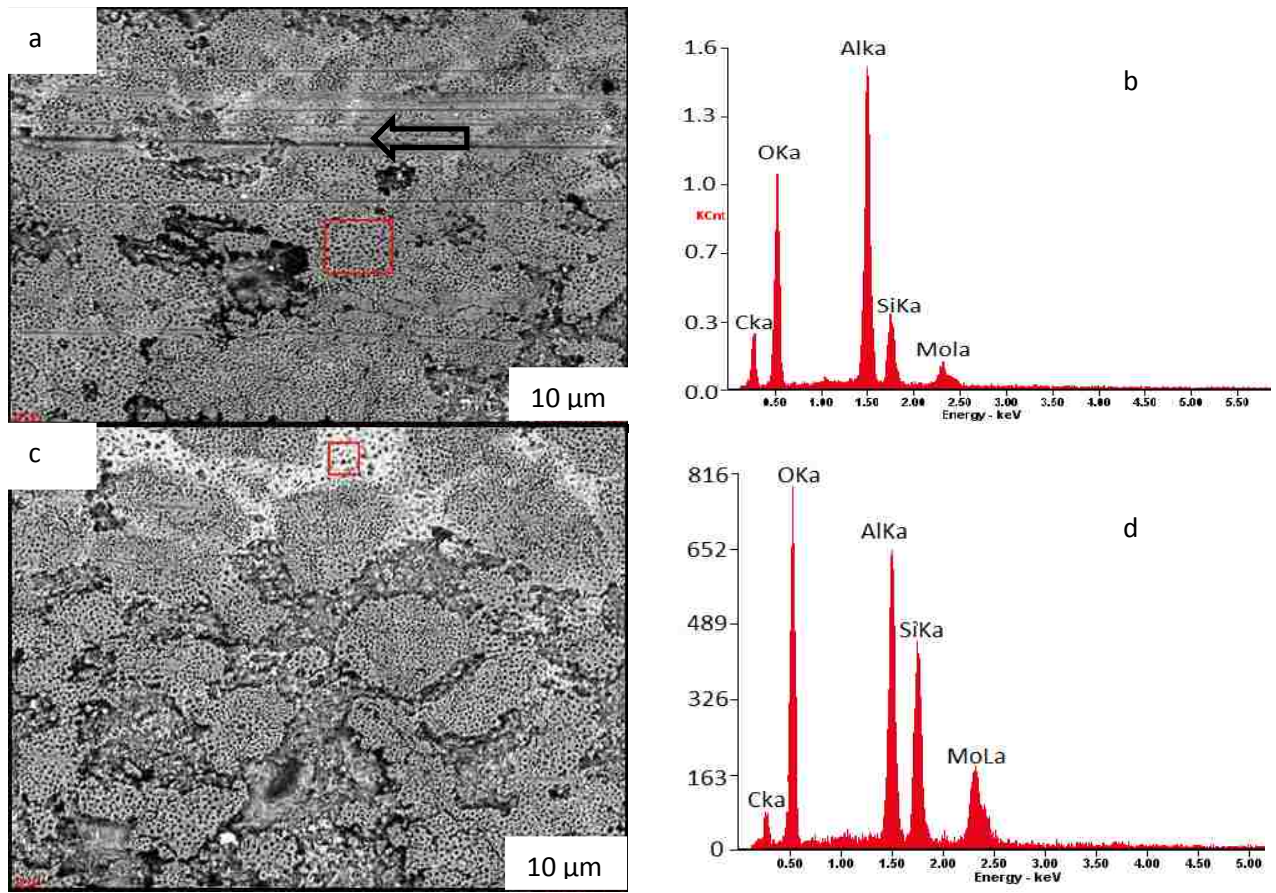


Fig. 7.5. SEM micrographs and EDX spectra of the coating S1 after tested at a 15N, 1000m and oil lubricant condition.

As mentioned before, even if the engine bore is always operated on the lubrication condition, there are still some cases for almost dry sliding of piston ring against the cylinder bore. Fig.7.6 shows the wear test result for selected PTWA sample and PEO coating (S1, prepared with long treatment time in a MoS_2 powder contained electrolyte). From the wear track pictures, it can be seen that under dry condition, the dimension for wear track on PTWA sample is much larger than the PEO sample. And also the C.O.F. value, Fig 7.6 (a), is higher than the PEO sample. Under a dry condition, the PTWA coated bore may be severely scratched by piston ring. On the other side, solid lubricant powders can play an important part for reducing the friction. Usually

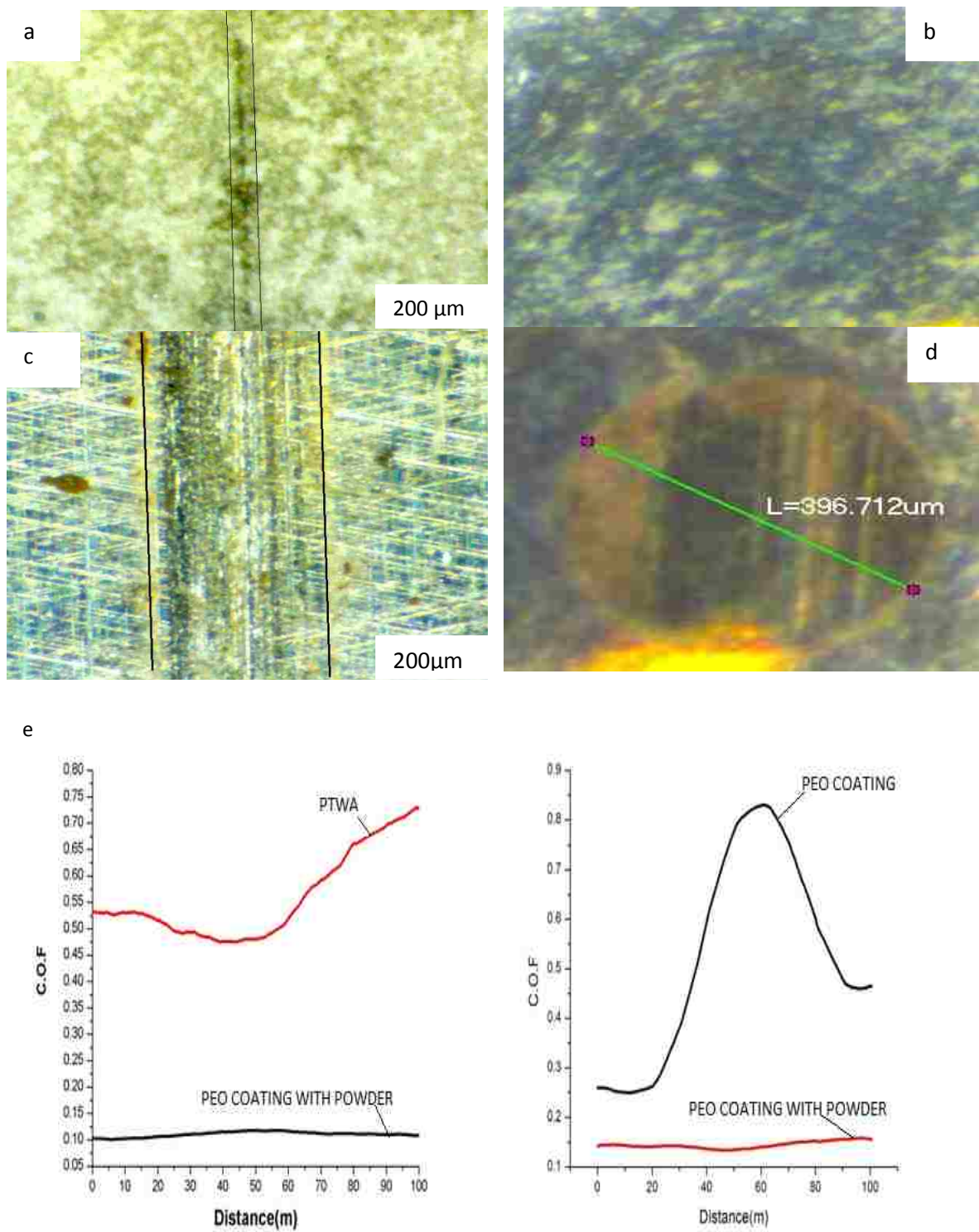


Fig. 7.6. Optical images of (a) the coating S1 and (b) counter-ball as well as (c) PTWA coating and (d) counter-ball. (e) C.O.F curves for the coatings.

the C.O.F. of a traditional PEO coating (as the coating S3) under dry condition is average 0.6. However, when the powders were added during the PEO process, the C.O.F. was dropped down to 0.15 which would significantly increase the anti-wear performance of the PEO coating under dry condition.

4. Conclusion

In this study, oxide coatings were deposited on cylinder bores made by a cast Al–Si alloy. The oxide coatings prepared in a MoS₂ powder-contained electrolyte appeared to have an improved tribological property. Incorporation of molybdenum and/or solid lubricant particles into the top oxide layer provided not only low friction to the coated Al–Si alloy but also good compatibility to the steel counterfaces. The counterface wear was related to the hardness and roughness of sample surfaces. The harder and rougher PEO coatings exhibited a higher degree of ball wear than the PTWA coating, but the PEO coatings had a lower coefficient of friction at both dry and oil lubricating test conditions. A better surface finish of a PEO coating would further improve the compatibility to steel counterface. Compared with all the PTWA, Alusil® and casting iron reference materials as a benchmark, the coefficients of friction of the PEO coatings were evenly low without spikes, and wear and plastic deformation of the coatings were minimal. The suddenly increased C.O.F (spikes) for tests of the commercially-used metallic based coating (PTWA) and bore materials (Alusil and cast iron) suggest that the reference materials were degraded during the accelerated test conditions. However, the even C.O.F. curves without a spike indicate the PEO coatings had a better resistance to scuffing wear. Therefore, the Mo-contained PEO coatings can be good candidates for engine cylinder bore surface protection.

References

- [1] E. Köhler, J. Niehues, in: K.U. Kainer, *Metal Matrix Composites Custom-made Materials for Automotive and Aerospace Engineering*, 1st ed., Wiley-VCH, Weinheim, 2006, pp. 95–108.
- [2] P. Krug, M. Kennedy, J. Foss, *SAE Int.* (2006), 2006-01-0983.
- [3] H. Ye, *JMEPEG* 12 (3) (2003) 288–297.
- [4] H. Ye, *JMEPEG* 12 (3) (2003) 288–297.
- [5] J. Zhang, A.T. Alpas, *Mater. Sci. Eng. A160* (1993) 25–35.
- [6] J. Zhang, A.T. Alpas, *Acta Mater.* 45 (2) (1997) 513–528.
- [7] A.D. Sarkar, *Wear* 31 (1975) 331–343.
- [8] J. Clarke, A.D. Sarkar, *Wear* 54 (1979) 7–16.
- [9] M. Chen, T. Perry, A.T. Alpas, *Wear* 263 (2007) 552–561.
- [10] A.R. Riahi, T. Perry, A.T. Alpas, *Mater. Sci. Eng. A343* (2003) 76–81.
- [11] F.A. Davis, T.S. Eyre, *Tribo. Int.* 27 (1994) 171–181.
- [12] A. Mahato, A.K. Sachdev, S.K. Biswas, *Wear* 265 (5–6) (2008) 849–855.
- [13] M. Dienwiebel, K. Pöhlmann, M. Scherge, *Tribo. Int.* 40 (2007) 1597–1602.
- [14] H. Kurita, H. Yamagata, H. Arai, T. Nakamura, *SAE Int.* (2004), 2004-01-1028.
- [15] B.E. Slattery, T. Perry, A. Edrissy, *Materials Science and Engineering A* 512 (2009) 76 – 81
- [8] A.L. Yerokhin, X. Nie, A. Leyland, A. Matthews, *Surf. Coat. Technol.* 130 (2000) 195.
- [9] F. Jaspard-Mecuson, T. Czerwiec, G. Henrion, T. Belmonte, L. Dujardin, A. Viola, J. Beauvir, *Surf. Coat. Technol.* 201 (2007) 8677.
- [10] X. Nie, E.I. Meletis, J.C. Jiang, A. Leyland, A.L. Yerokhin, A. Matthews, *Surf. Coat. Technol.* 149 (2002) 245.
- [11] A.L. Yerokhin, A. Shatrov, V. Samsonov, P. Shashkov, A. Leyland, A. Matthews, *Surf.*

Coat. Technol. 182 (2004) 78.

[20] A.L. Yerokhin, X. Nie, A. Leyland, A. Matthews, S.J. Dowey, Surf. Coat. Technol. 122 (1999) 73

[21] P. Bala Srinivasan, J. Liang, C. Blawert, W. Dietzel, Appl. Surf. Sci. 256 (2010) 3265.

[22] Y. Han, J. Song, J. Am. Ceram. Soc. 92 (2009) 1813.

[23] P. Bala Srinivasan, C. Blawert, W. Dietzel, Wear 266 (2009) 1241.

[24] X.P. Zhang, Z.P. Zhao, J. Mater. Sci. 42 (2007) 8523.

[25] J. Guo, L. Wang, J. Liang, Q. Xue, F. Yan, J. Alloy. Compd. 481 (2009) 903.

[26] Tongbo Wei, Fengyuan Yan*, Jun Tian, Journal of Alloys and Compounds 389 (2005) 169–176

[27] Jun Feng Su, Xueyuan Nie, Henry Hu, and Jimi Tjong J. Vac. Sci. Technol. A 30, 061402 (2012)

[28] Y. Ma, X. Nie, D.O. Northwood, H. Hu, Thin Solid Films 469–470 (2004) 472.

[29] A.L. Yerokhin, A. Shatrov, V. Samsonov, P. Shashkov, A. Leyland, A. Matthews, Surf. Coat. Technol. 182 (2004) 78.

[30] S. Wilson, A.T. Alpas, Wear 212 (1997) 41.

[31] H. Guo, M. An, Appl. Surf. Sci. 246 (2005) 229–238.

[32] H. Duan, K. Du, C. Yan, F. Wang, Electrochim. Acta 51 (2006) 2898–2908.

[33] A. Erdemir, Tribol. Int. 38 (2005) 249–256.

[34] J. Guo, L. Wang, J. Liang, Q. Xue, F. Yan, Journal of Alloys and Compounds 481(2009) 903-909

[35] M. Hahn, R. Theissmann, B. Gleising, W. Dudzinski, A. Fischer, Wear 267 (2009) 916–924

[36] M. Dienwiebel, K. Pohlmann, M. Scherge, Tribology International. 40 (2007) 1597–1602

[37] Fairhurst W, Rohrig K. Abrasion resistance high–chromium white cast irons 1989.

[38] Metals handbook, 9th ed. 15 Casting; 1988.

[39] S.Yajsar, Investigation of wear and microstructure of turbine pallet of sanding machine.

M.Sc. Thesis, Institute of Science and Technology, Gazi University; 2001.

Chapter 8

Summary and future work

1. Summary

Linerless aluminium engine block cylinder bore surfaces need coatings to prevent wear and corrosion problems. In this thesis, plasma electrolytic oxidation coating technology was used to produce oxide coatings on an aluminium alloy A356. The uncoated A356 and commercially-used cylinder bore materials were also used for comparison study. The oxide coatings were to provide corrosion and wear resistance of the A356 alloy for aluminium engine applications. The coatings' corrosion property was tested in an E85 alternative fuel medium. The tribological properties of the coatings were tested in dry and lubricating conditions. To reduce coefficient of friction of the oxide coatings against steel counter face materials, the coatings were also prepared in an electrolyte containing MoS₂ powders. The modified coatings showed to possess a lower coefficient of friction, which would increase fuel efficiency when the coatings are used on engine cylinder bore surfaces. The results are summarized as follows.

I. Corrosion property of Plasma Electrolytic Oxidation (PEO) coatings tested in an ethanol-gasoline fuel (E85) medium

Ceramic oxide coatings were prepared on an engine bore material: aluminum A356 alloy by a plasma electrolytic oxidation (PEO) technique under unipolar, bipolar and duplex unipolar/bipolar current modes. Cross-sectional morphologies of the coatings were studied using a scanning electron microscope (SEM). The corrosion behavior of the coated and uncoated

samples was evaluated in ethanol-gasoline E85 fuels through potentiodynamic polarization and zero resistance ammeter (ZRA) testing methods. The results indicated that all the coatings had a better corrosion resistance compared to the uncoated substrate. The unipolar current mode created the PEO coating with a thicker coating microstructure and thus a better corrosion resistance, compared to a bipolar current mode. The duplex treatments of unipolar/bipolar or bipolar/unipolar current modes produced an even better performance of the coatings against galvanic corrosions caused by a steel/Al coupling in the E85 fuel medium.

II. Corrosion property of contacts between carbon fiber cloth materials and typical metal alloys with and without Plasma Electrolytic Oxidation (PEO) coatings

The demand for the use of carbon-fiber-reinforced materials in automotive industry is increasing worldwide. A destructive galvanic corrosion is inevitable when carbon fiber contacts with metals. In this research, the galvanic corrosion between carbon fiber and three kinds of commonly used metals, A356 aluminum alloy and Ti6Al4V titanium alloy, was studied. By employing the potentiodynamic polarization tests and zero resistance ammeters testing (ZRA) method, the corrosion potential and their differences in values were analyzed in a 3.5% NaCl solution. It was found that when coupled with carbon fiber, steel and A356 aluminum alloy were corroded while the titanium alloy remained almost intact. To address this problem for the lightweight aluminum alloys, the plasma electrolytic oxidation (PEO) technique was again employed to synthesize oxide coatings on the A356 alloy and Ti6Al4V titanium alloy as well. The results of the experiments showed the rate of the galvanic corrosion current could be decreased significantly when the PEO coatings were applied on the aluminum surfaces. The coatings prepared using

duplex unipolar and bipolar treatments had a dense surface and as a result, showed the lowest corrosion current and highest corrosion resistance in the polarization corrosion and ZRA tests. For the Ti-6Al-4V cases, both coated and uncoated samples exhibited excellent galvanic corrosion resistances in the test environment.

III. MoS₂/Al₂O₃ composite coatings on A356 alloy

In order to reduce the fuel consumption and pollution, automotive companies are developing low friction surface technologies. Plasma electrolytic oxidation (PEO) is a promising surface modification techniques for the improvement of the tribological properties of metals, such as Al, Mg, Ti and their alloys. In this research, a plasma electrolytic oxidation (PEO) ceramic coating process was used to form ceramic MoS₂ oxide composite coatings on aluminum with intention for lower friction. The tribological properties of the oxide-MoS₂ coatings were evaluated by sliding wear tests under the dry and lubricate conditions at the room temperature. The test results showed that the solid lubrication MoS₂ can be integrated into the coatings for friction reduction. The role of solid lubrication in reducing friction coefficient has been exhibited more significantly in the oil test condition than in the dry test condition.

IV. Plasma electrolytic oxidation coatings on engine bores to modify friction and wear behavior

Since most conventional aluminum (Al) alloys have poor wear resistance, various technical solutions have been developed to generate wear-resistant cylinder bores against the sliding piston ring. In this work, the plasma electrolytic oxidation (PEO) process was employed to produce oxide ceramic coatings on an Al alloy A356 for Al engine block applications, to protect against

the wear damage. A reciprocating sliding tribometer was used to investigate the tribological and wear behavior of the PEO coatings and counterface materials under dry and lubricated conditions. A hypereutectic Al-Si alloy (Alusil), cast iron and plasma transferred wire arc (PTWA) coatings were also tested for the comparison study. The results show that the PEO coating can have a low coefficient of friction and minimal wear. The special PEO coating with some additive powders can be used as an alternative coating for wear and friction reduction of Al cylinder bores.

2. Future work

The corrosion experiments were conducted in room temperature and the A356 material was Ingot casting condition (large grain sizes). The future corrosion study in E85 should be also done at elevated temperatures to simulate the engine combustion conditions. The influence of grain sizes of the alloy's microstructure on coating preparation and properties is needed in the future study as well. There is also a need to find appropriate ways to increase amount of MoS₂ powders in the oxide coatings for further friction reduction.

COPYRIGHT RELEASES FROM PUBLICATIONS

Zhijing Peng <peng7@uwindsor.ca>

to permissions

Dear Sir :

I am completing a Master Thesis at the University of Windsor entitled " Plasma Electrolytic Oxidation (PEO) Coatings on an A356 Alloy for Improved Corrosion and Wear Resistance"

I would like your permission to include in my thesis the following material:

Z. Peng, X. Nie * "Galvanic corrosion property of contacts between carbon fiber cloth materials and typical metal alloys in an aggressive environment" Surface & Coatings Technology 215 (2013) 85–89

My thesis will be deposited to the University of Windsor Leddy library or University of Windsor 's online theses and dissertations repository (<http://winspace.uwindsor.ca>) and will be available in full-text on the internet for reference, study and / or copy. I will also be granting Library and Archives Canada and Pro Quest/UMI a non-exclusive license to reproduce, loan, distribute, or sell single copies of my thesis by any means and in any form or format. These rights will in no way restrict republication of the material in any other form by you or by others authorized by you.

Please confirm in writing or by email that these arrangements meet with your approval.

Thank you very much for your attention to this matter.

Sincerely, Zhijing Peng Master . Candidate,
Dept. of Mechanical, Automotive, & Materials Engineering
University of Windsor
401 Sunset Avenue
Windsor, Ontario, N9B 3P4
Phone: [\(519\) 980 8688](tel:5199808688)

PLEASE READ - IMPORTANT INFORMATION ON OBTAINING PERMISSION

Rights and Permissions (ELS)

to me

Thank you for your email. If you are requesting to re-use content from any publication found on <http://www.ScienceDirect.com>, Elsevier requires that you follow the directions below to obtain permission.

Please understand that Elsevier will **not** reply to your permission request if the publication you wish to use content from is available on ScienceDirect.

IF THE CONTENT YOU WISH TO USE IS AVAILABLE ON SCIENCEDIRECT, PLEASE FOLLOW THESE INSTRUCTIONS:

- Locate the publication containing your desired content on <http://www.sciencedirect.com/science/jrnllallbooks>
- Click on the article/chapter name to access the abstract
- Directly below the article title on the left, click “Permissions & Reprints”
- The Rightslink request page will then be launched (please disable your pop-up blocker)
- Select the way you would like to reuse the content
- Create a Rightslink account if you haven’t done so already
- Accept the terms and conditions and you’re done

Please note that certain requests may require review before a license to reuse is available; should this occur, you will be emailed to accept or decline the fee and/or terms of the license as set by Elsevier’s Global Rights Department upon review.

For questions about using the Rightslink service, please contact Customer Support via phone - US [877/622-5543](tel:8776225543) (toll free) or [978/777-9929](tel:9787779929) 8:00 am – 6:00 pm Eastern Time, or email customercare@copyright.com.

IF THE CONTENT YOU WISH TO USE IS NOT AVAILABLE ON SCIENCEDIRECT OR YOU HAVE SUBMITTED A QUESTION/QUERY, PLEASE NOTE THE FOLLOWING:

- The Elsevier Global Rights team will review your request/email and respond within 15 working days unless you have specified a more immediate deadline.
- You should not reply to this automated response. Should you need to follow up on your request please ensure you attach it to any correspondence.

- Please verify that the content you wish to use is not available online before awaiting a response to your email.

For general questions about obtaining permission, please contact the Permissions Helpdesk at permissionshelpdesk@elsevier.com or US [800/523-4069 x 3808](tel:8005234069) (toll free).

Kind regards,

Global Rights Department

Tel: [+44 \(0\)1865 843830](tel:+4401865843830) (UK) or [+ 1 215 239 3804](tel:+12152393804) (US)

Email: permissions@elsevier.com



Title: Galvanic corrosion property of contacts between carbon fiber cloth materials and typical metal alloys in an aggressive environment

Author: Z. Peng,X. Nie

Publication: Surface and Coatings Technology

Publisher: Elsevier

Date: 25 January 2013

Copyright © 2013, Elsevier

Logged in as:
Zhijing peng

[LOGOUT](#)

Order Completed

Thank you very much for your order.

This is a License Agreement between Zhijing peng ("You") and Elsevier ("Elsevier"). The license consists of your order details, the terms and conditions provided by Elsevier, and the [payment terms and conditions](#).

[Get the printable license.](#)

License Number	3083150580579
License date	Feb 06, 2013
Licensed content publisher	Elsevier
Licensed content publication	Surface and Coatings Technology
Licensed content title	Galvanic corrosion property of contacts between carbon fiber cloth materials and typical metal alloys in an aggressive environment
Licensed content author	Z. Peng,X. Nie
Licensed content date	25 January 2013

Licensed content volume number	215
Number of pages	5
Type of Use	reuse in a thesis/dissertation
Portion	full article
Format	both print and electronic
Are you the author of this Elsevier article?	Yes
Will you be translating?	No
Order reference number	
Title of your thesis/dissertation	Plasma Electrolytic Oxidation (PEO) Coatings on an A356 Alloy for
Expected completion date	Feb 2013
Estimated size (number of pages)	150
Elsevier VAT number	GB 494 6272 12
Permissions price	0.00 USD
VAT/Local Sales Tax	0.00 USD
Total	0.00 USD

----- Original-Nachricht -----

Betreff: Request for permission to include the paper in my thesis

Datum: Tue, 5 Feb 2013 10:08:07 -0500

Von: Zhijing Peng <peng7@uwindsor.ca> <mailto:peng7@uwindsor.ca>

An: info@scientific.net

Dear Sir :

I am completing a Master Thesis at the University of Windsor entitled "
Plasma Electrolytic Oxidation (PEO) Coatings on an A356 Alloy for Improved
Corrosion and Wear Resistance"

I would like your permission to include in my thesis the following material:

Zhijing Peng, Tse Cheng, Xueyuan Nie "MoS₂/Al₂O₃ composite coatings on
A356 alloy for friction reduction" Advanced Materials Research Vol
496 (2012) pp 488-492

Zhijing Peng , Ying Chen and Xueyuan Nie,* " Corrosion properties of plasma electrolytic oxidation ceramic coatings on an A356 alloy tested in an ethanol-gasoline fuel (E85) medium" Advanced Materials Research Vols. 282-283 (2011) pp 774-778

My thesis will be deposited to the University of Windsor Leddy library or University of Windsor 's online theses and dissertations repository (<http://winspace.uwindsor.ca>) and will be available in full-text on the internet for reference, study and / or copy. I will also be granting Library and Archives Canada and Pro Quest/UMI a non-exclusive license to reproduce, loan, distribute, or sell single copies of my thesis by any means and in any form or format. These rights will in no way restrict republication of the material in any other form by you or by others authorized by you.

Please confirm in writing or by email that these arrangements meet with your approval

Thank you very much for your attention to this matter.

Sincerely,

Zhijing Peng Master . Candidate,

Dept. of Mechanical, Automotive, & Materials Engineering

University of Windsor

401 Sunset Avenue Windsor, Ontario, N9B 3P4 Phone: (519) 980 8688

Dear Zhijing Peng,

Thank you for your email. This is okay with us. Please include proper information where the original was published.

Best wishes for your Master Thesis,

Thomas Wohlbier

Thomas Wohlbier

Director of Publications & CCO

Trans Tech Publications

105 Springdale Lane

Millersville, PA 17551

U.S.A.

Email: t.wohlbier@ttp.net

Fax: +1 717 872 4327

Trans Tech Publications

Kreuzstr. 10

8635 Zurich-Durnten.

Switzerland

Fax +41 44 922 1033

<http://www.ttp.net>

<http://www.scientific.net>

Zhijing Peng <peng7@uwindsor.ca>

to jcheng

Dear Dr. Tse.Cheng

Can I use paper *Zhijing Peng, Tse Cheng and Xueyuan Nie, MoS₂/Al₂O₃ composite coatings on A356 alloy for friction reduction.*

Advanced Materials Research, Vol. 496 (2012) pp 488-492 as one chapter in my thesis?

Thanks

zhijing Peng

2013-2--27

.Reply .Forward



Tse Cheng jcheng@uwindsor.ca

to **peng7**

Dear Zhijing,

Yes, you can use it without any problem.

Tse Cheng

2013-2-27

Zhijing Peng <peng7@uwindsor.ca>

to chen111w

Dear Dr.Chen

Can I use paper Zhijing Peng, Ying Chen and Xueyuan Nie, Corrosion properties of plasma electrolytic oxidation ceramic coatings on an A356 alloy tested in an ethanol-

gasoline fuel (E85) medium. Advanced Materials Research, Vols. 282-283 (2011) pp

774-778 as one chapter in my thesis?

Thanks

zhijing Peng

2013-2-27

.Reply .Forward



Ying Chen <chen111w@uwindsor.ca>

to me

Hi, Mr. Peng

Yes, you can use the paper published in Advanced Materials Research, Vols. 282-283 (2011) pp 774-778 .

Good luck!

VITA AUCTORIS

NAME: Zhijing Peng
PLACE OF BIRTH: Beijing, China
YEAR OF BIRTH: 1979
EDUCATION: University of Windsor, Canada
2004-2008, B.Sc
University of Windsor, Canada
2011-2013, M.A.Sc